ON THE POSTBUCKLING BEHAVIOR OF A THIN SHEET WITH A CIRCULAR HOLE IN A UNIDIRECTIONAL TENSILE FIELD

A THESIS

Presented to

The Faculty of the Division of Graduate

Studies and Research

by

Abraham Samuel Hananel

In Partial Fulfillment

of the Requirements for the Degree

Doctor of Philosophy

in the School of Aerospace Engineering

Georgia Institute of Technology

January 1974

ON THE POSTBUCKLING BEHAVIOR OF A THIN SHEET WITH A CIRCULAR HOLE IN A UNIDIRECTIONAL TENSILE FIELD

Approved:

Robert L. Carlson, Chairman

Jerry M. Anderson

C. Virgil Smith, Jr.

Date approved by Chairman: 1-24-74

ACKNOWLEDGMENTS

My unreserved gratitude is extended to Dr. Robert L. Carlson, my thesis advisor, for his ideas and guidance during the course of this research and for the numerous hours of fruitful consultation, which often extended into the evening. Dr. Carlson's ready availability for discussions and his effectively helpful attitude in all matters played a very important role in the development and completion of my dissertation.

I wish to express my sincere thanks and appreciation to Dr. C. Virgil Smith for his deep involvement in my dissertation, as main reader, and for his precise comments and suggestions. I also wish to thank Dr. Jerry M. Anderson and the other members of the reading committee, Dr. Sathyanarayana V. Hanagud and Dr. James I. Craig, for their essential contributions.

I would like to thank the Lockheed-Georgia Company Management, and the C-5 Project Management in particular, for the help extended to me during my studies, in the form of the Graduate Work-Study Program.

Mrs. Ruth Shaw deserves my very special thanks for her virtuoso typing of this manuscript and for the considerate arrangements she made during our collaboration.

TABLE OF CONTENTS

		Page
ACKNOWLEDGMENTS		ii
LIST OF TABLES		v
LIST OF FIGURES		vi
NOMENCLATURE		vii
SUMMARY		xiv
Chapter		
I.	INTRODUCTION	1
	General Objective	
II.	GOVERNING EQUATIONS	8
	General Equilibrium Equations Stress-Strain Equations Strain-Displacement Equations The von Karman Plate Equations in Cylindrical Coordinates	
III.	PREPARATORY ANALYSIS	21
	Derivation of the Total Potential The Strain Energy of the Plate The Potential of the External Loads Selection of Displacement Functions Determination of the Radial and the Circumferential Variables Derivation of In-Plane Displacements	

Chapter Page

IV. SOLUTION 42

General
Derivation of the System of Matrix Equations
Initial Values for $\{a_i\}$ and $\{c_k\}$
Alternatives for the Non-Linear Solution
An Iteration Process
A Successive Approximation Approach
A Perturbation Approach

V. RESULTS 55

General
The Associated Eigenvalue Problem
Solution to the Non-Linear Problem
Conclusions
Recommendations for Future Research

APPENDIX

A. APPLICATION OF KIRCHHOFF'S HYPOTHESIS TO THE NON-LINEAR PLATE PROBLEM 71

B. EXPRESSIONS FOR THE MATRICES USED IN CHAPTER IV . . 75

C. INTEGRALS USED IN EVALUATING THE MATRIX ELEMENTS IN CHAPTER IV 81

D. A PERTURBATION APPROACH 84

REFERENCES 92

VITA 94

LIST OF TABLES

Table		Page
1	Values of λ with $\alpha = 1/10$ and 20 x 20 Terms for u and 20 x 1 Terms for v	57
2	Values of λ with $\alpha = 1/10$ and 10 x 2 Terms for u and 10 x 1 Terms for v	58
3	Effect of $\alpha = \frac{a}{b}$ on the Plane Stress State, with 10 x 2 Terms for u and 10 x 1 Terms for v . .	59
4	Effect of Number of Terms for u and v on the Plane Stress State, with $\alpha = 1/10$	60
5	Effect of Number of Terms for u and v on the Plane Stress State, with $\alpha = 1/20$	60
6	Eigenvectors corresponding to Eigenvalues in Table 1. Values of $\overset{0}{\xi}_k$	63
7	Eigenvectors Corresponding to Eigenvalues in Table 2. Values of $\overset{0}{\xi}_k$	64

LIST OF FIGURES

Figure		Page
1	Circular Plate with Circular Hole	4
2	Load-Deflection Curve for Given r and θ	7
3	Transverse Deflection at the Hole Boundary	65
4	Tensile Stress Concentration Factor vs the Transverse Deflection	66
5	Compressive Stress Concentration Factor vs the Transverse Deflection	66
A1	Kirchhoff's Hypothesis	72

NOMENCLATURE

A	area of plate
a	radius of inner boundary of plate
a_i	coefficients associated with the in-plane displacements u and v
a_{mn}	double-indexed form of the coefficients a_i
$\{a\}$	column matrix of the coefficients a_i
B	bending strain energy per unit area of plate
$[B]$	real symmetric matrix
b	radius of outer boundary of plate
b_j	coefficients associated with the circumferential in-plane displacements v
b_{ij}	components of the material constants tensor
c_k	coefficients associated with the transverse displacements w
$\{c\}$	column matrix of the coefficients c_k

D	bending stiffness of plate, $Et^3/12(1-\nu^2)$
E	Young's modulus
E'	$E(1-\nu^2)$
e_{ij}	components of the general strain tensor
f	integer
$\{g\}$	column matrix derived from the energy of the external loads
g^{ij}	components of the metric tensor
$[H]$	real symmetric matrix
h^i_{jk}	auxiliary symbol identical to 1
I, I'	integers
I_1, I_2	strain invariants
$[I]$	identity matrix
i	integer
J	integer
j	integer

$\bar{j}_r, \bar{j}_\theta, \bar{j}_z$	directional unit vectors in the cylindrical coordinate system
K	integer
k	integer
ℓ	integer
M	membrane strain energy per unit area of plate
$[M]$	real symmetric matrix
m	integer
N	integer
N_r	radial stress resultant
N_θ	circumferential stress resultant
$N_{r\theta}$	shear stress resultant
$\bar{N}_r$	N_r for r = b
$\bar{N}_{r\theta}$	$N_{r\theta}$ for r = b
n	integer
$\bar{n}$	vector used in Appendix A

p	integer
q	integer
$\bar{r}$	radius vector
r	radial coordinate in the cylindrical system; radius
S	applied uniform stress
T	strain energy per unit area of plate
t	plate thickness
U	radial component of the displacement vector; also, total strain energy of plate
U_o	strain energy density of plate
U_B	bending strain energy of plate
U_M	membrane strain energy of plate
$\bar{U}$	displacement vector
u	in-plane radial displacement
u^o	flat plate radial displacement
u^i	radial displacement mode; also, contravariant displacement component

u_i	covariant displacement component
V	circumferential component of the displacement vector
v	in-plane circumferential displacement
v^o	flat plate circumferential displacement
v^j	circumferential displacement mode
W, w	transverse component of the displacement vector
w^k	transverse displacement mode
$[X]$	real non-symmetric matrix
x	variable of integration (Appendix C); also, integer (Appendix B)
y	integer (Appendix B)
z	axial coordinate in the cylindrical system; also, integer (Appendix B)
α	the ratio a/b; also, integer
β	integer
Γ^i_{jk}	Euclidean Cristoffel symbol
γ	integer

ε_{ij}	physical components of the strains e_{ij}
ε_{rr}	radial strain
$\varepsilon_{\theta\theta}$	circumferential strain
$\varepsilon_{r\theta}$	shear strain
θ	circumferential coordinate in the cylindrical system
λ	Lamé constant; also, load parameter, Sa^2t/D or $2\alpha^2/\omega$
λ_o	smallest positive value for λ
μ	Lamé constant-shear modulus
ν	Poisson's ratio
π	total potential of plate
ρ	radial variable, $1 - r/b$
σ_r	radial plate stress
σ_θ	circumferential plate stress
τ	shear plate stress
ϕ	Airy stress function

Ω	potential of the external loads
ω	real eigenvalue, $2D/Sb^2t$
ω_o	largest positive value for ω
∇^4	square Laplacian operator ∇^2

SUMMARY

A perfectly flat, tensioned sheet with a circular hole can undergo out-of-plane deflection if the applied load exceeds a critical value. Although the buckled sheet can support loads above the critical value, the redistribution of the stresses in the sheet, especially around the hole, can be expected to affect both the fatigue and the ultimate load capacity.

This behavior of the plate is governed by a system of three non-linear differential equations in the displacements u, v and w. These are the von Karman equations in the displacement formulation. An approximate solution for the displacements is obtained using the Ritz method. By making stationary the total potential of the plate with respect to the constant coefficients in the assumed expressions for the displacements, two coupled matrix equations are derived with non-linear terms in the coefficients, which are solved by a perturbation technique.

Stresses are evaluated at the plate faces as well as at the midsurface of the plate for several locations of stress concentration around the hole. The effect of the large transverse deflections is evident from the redistribution of the stresses in the plate.

CHAPTER I

INTRODUCTION

General

When a uniform uniaxial finite stress is applied to a plate containing a hole, the stress at some point or points at the edge of the hole will exceed the applied stress by a factor which is called the Stress Concentration Factor. (SCF for short). The earliest investigation of this effect was reported by G. Kirsch three quarters of a century ago, in 1898 (Ref. 1). Kirsch analysed the stress distribution in an infinite linearly elastic plate with a centered circular hole under uniaxial tension. Thirty one years later, in 1929, R. C. J. Howland (Ref. 2) published his solution for the finite width strip with a centered circular hole.

In both the above cases, as well as in the vast majority of the subsequent investigations, the plate was assumed to remain flat, i.e., no transverse displacements were considered. There has been a number of solutions, though, in which the material was assumed to behave differently from the linearly elastic one considered by Kirsch and Howland. Selected examples of analyses involving stress concentration are given below, starting with the basic case of linearly elastic material.

(1) The material is linearly elastic. The plane stress solution for an infinite plate (the Kirsch solution) yields a SCF of 3 in

tension and SCF of -1 in compression. This solution is valid so long as 3S (S = applied tensile stress) does not exceed the elastic limit of the material. In the case of the finite width strip (the Howland solution) the SCFs are higher than the numbers cited above, and they increase with the decrease in width (Ref. 2, p. 74).

(2) The material is non-linearly elastic with decreasing stiffness. The plane strain solution for such materials yields SCFs lower than the ones from the Kirsch solution, and the SFCs decrease with the increase in the applied tension S. This solution is due to Adkins, Green and Shields (Ref. 3, p. 210).

(3) The material is linearly elastic up to a limit, beyond which it becomes perfectly plastic. The tension SCF will be 3 until the peak stress reaches the plastic limit. When the applied tension S exceeds 1/3 of the plastic stress limit for the material, a stress redistribution takes place, and it is found that the peak stress remains constant and equal to the plastic limit. The stress in the rest of the plate increases. In this manner the SCF can be reduced considerably below 3.

(4) The material creeps non-linearly. Under a tensile stress of long duration the material undergoes deformations which are functions of the local stress history. The material at the highly stressed areas will flow and the stress distribution tends to become more uniform. This results in a reduction in the stress concentration factor (Ref. 4, p. 58).

An avenue of investigation different from the preceding examples would be to allow geometric non-linearities, while retaining the

linearly elastic material. All the cases enumerated above have one common feature, i.e., they are all variations of the basic two dimensional problem. If the assumption that the plate remains flat under the tension is discarded, and the plate is allowed to undergo finite, moderately large transverse deflections, it becomes possible to investigate a new practical aspect of the stress concentration problem. The SCF will have the value corresponding to the flat plate until the applied tensile stress reaches a sufficiently high value; at this value for the tension the hole boundary becomes unstable and buckling occurs. This buckling, which involves finite deflections, should cause a change in the SCF at the midsurface of the plate as compared to the results of the two-dimensional solution. Such a comparison will, however, be incomplete if only membrane stresses are taken into account. The finite deflections of the plate will give rise to bending stresses, which will further modify the SCF when evaluated away from the midsurface of the plate.

Objective

The main objective of the investigation described in this dissertation is to determine the stress distribution and the deflection modes for a thin plate of large dimensions with a circular hole and having a uniformly applied tension on two opposite edges (see Fig. 1). For a sufficiently large stress local buckling will occur. This value of the stress is determined at the first step of the solution of the system of non-linear coupled equations to which the solution of the problem at hand is reduced (see Chapter IV). This first step is

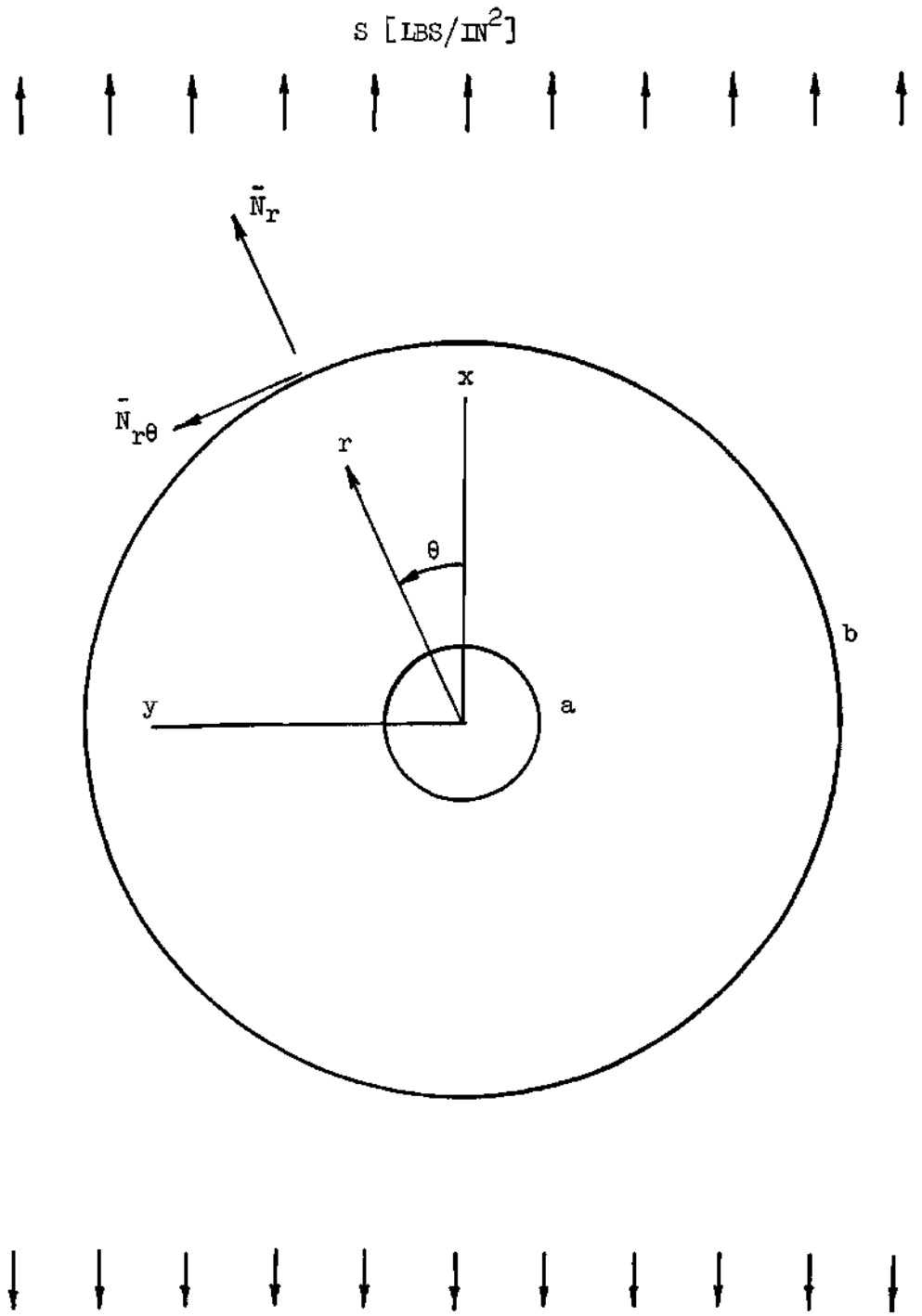

Figure 1. Circular Plate with Circular Hole

equivalent to the solution of an eigenvalue problem. The postbuckling behavior of the plate (stress distribution and deflections) must be determined by a solution of a non-linear problem based on the von Karman plate theory. This theory makes the following assumptions (Reference 5, p. 463):

(1) The magnitude of the deflection w is of the same order of magnitude as the thickness t of the plate, but very small compared with the typical plate dimension L:

$$|w| = O(t) \quad \text{and} \quad |w| \ll L$$

(2) The slope of the surface of deflection is everywhere small:

$$\left|\frac{\partial w}{\partial x_1}\right| \ll 1 \quad \text{and} \quad \left|\frac{\partial w}{\partial x_2}\right| \ll 1,$$

where x_1 and x_2 are the in-plane variables.

(3) The in-plane displacements u (radial displacement) and v (circumferential displacement) are infinitesimal. In the strain-displacement relations only non-linear terms in $\partial w/\partial x_1$ and $\partial w/\partial x_2$ are retained. All other non-linear terms are neglected.

(4) The strain components are small and Hooke's law for an isotropic material holds.

(5) Every straight line originally normal to the plate mid-surface remains, after deformation, straight, normal to the deflected midsurface and of the same length as before the deformation (Kirchhoff's

hypothesis).

The postbuckling behavior of the plate at the inner boundary (i.e., the hole edge) will be described by reference to a load-deflection curve (see Figure 2). The deflection w will be a function of the applied stress S:

$$w = w(r, \theta; S)$$

A number of such load-deflection curves can be constructed for selected points on the inner boundary.

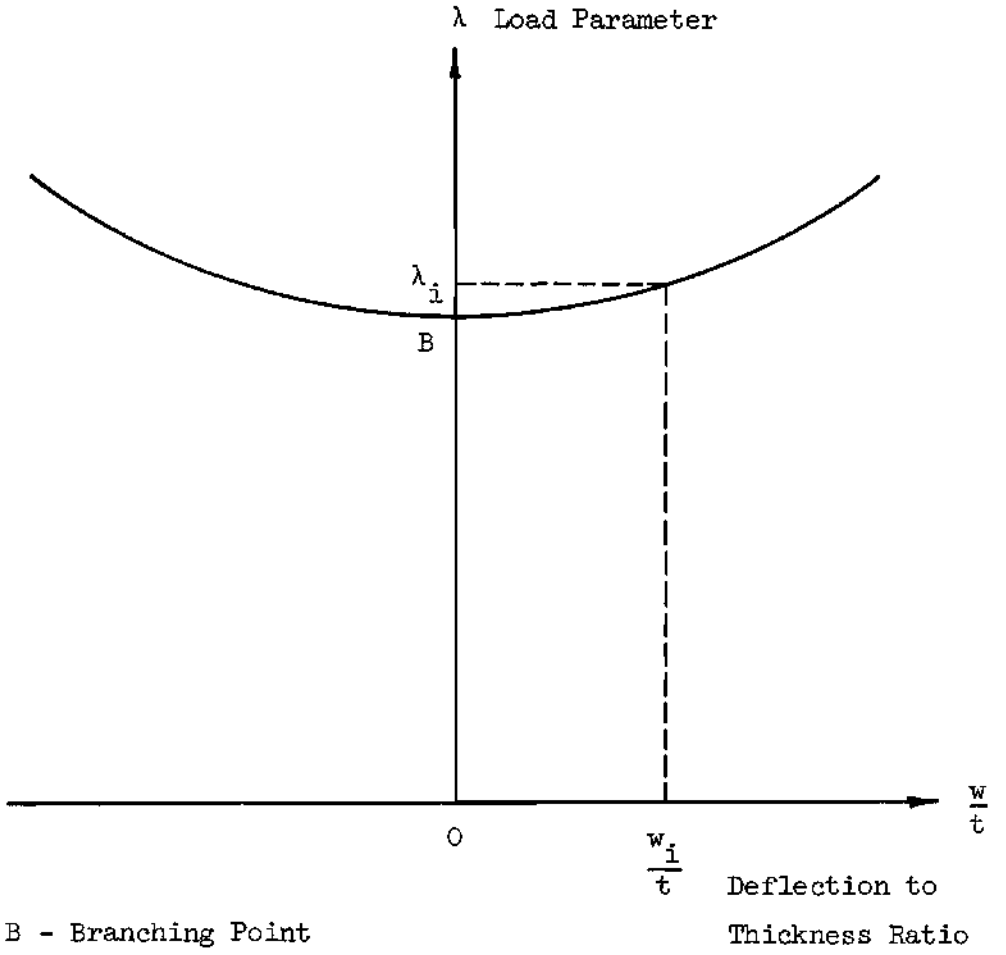

Figure 2. Load-Deflection Curve for Given r and θ.

CHAPTER II

GOVERNING EQUATIONS

General

The problem, as defined, will be solved by use of a displacement formulation. This means that there will have to be solved three equations in the three unknown displacements u, v and w. The stress formulation of the problem would have yielded only two equations in the unknowns w, the transverse displacement, and ϕ, the Airy stress function. But to use the stress formulation on a multiply connected body, ϕ must satisfy the three generalized Michell conditions for each internal boundary (Ref. 6, p. 425 and Ref. 7, p. 762). In using the displacement formulation, no such conditions need be considered.

Since the boundaries of the plate under consideration are circular, a cylindrical coordinate system will be used throughout the solution. The applied loads on the outer boundary will be derived from the uniaxially applied uniform stress S on two opposite edges of a rectangular plate of infinite dimensions (Ref. 8, p. 80); see also Figure 1.

Equilibrium Equations

The three equations which contain the three unknown displacements u, v, and w are the two in-plane equations of equilibrium

and the equation of transverse equilibrium. As per Reference 5, p. 115 and Reference 9, p. 45-14, for instance, we have:

Radial equilibrium -

$$\left(r\, N_r\right)_{,r} + N_{r\theta,\theta} - N_\theta = 0 \tag{1}$$

Circumferential equilibrium -

$$\left(r^2\, N_{r\theta}\right)_{,r} + r\, N_{\theta,\theta} = 0 \tag{2}$$

Transverse equilibrium -

$$D\nabla^4 w = w_{,rr}\, N_r + \frac{1}{r}\left(w_{,r} + \frac{1}{r}\, w_{,\theta\theta}\right) N_\theta + 2\left(\frac{w_{,\theta}}{r}\right)_{,\theta} N_{r\theta} \tag{3}$$

Here N_r, N_θ and $N_{r\theta}$ are the radial, circumferential and shear loads per unit length; $D = Et^3/12(1-\nu^2)$, where E is the Young modulus, ν is the Poisson ratio and t is the plate thickness,

The subscripts following the comma denote partial differentiation with respect to the variables represented by the subscripts.

Stress-Strain Equations

The stresses σ_r, σ_θ and τ are expressible in terms of the strains as follows (Ref. 10, p. 161):

Radial stress -

$$\sigma_r = E'\left(\epsilon_{rr} + \nu\, \epsilon_{\theta\theta}\right) \tag{4}$$

Circumferential stress -

$$\sigma_\theta = E'\left(\epsilon_{\theta\theta} + \nu\, \epsilon_{rr}\right) \tag{5}$$

Shear stress -

$$\tau = \left(1 - \nu\right) E'\epsilon_{r\theta} \tag{6}$$

where $E' = \frac{E}{1-\nu^2}$ and ϵ_{rr}, $\epsilon_{\theta\theta}$ and $\epsilon_{r\theta}$ are the radial, circumferential and shear strains (i.e., the physical components of the strain tensor).

Equations (4), (5) and (6) follow from the condition of plane stress ($\sigma_{zz} = 0$) and from the assumption that the plate material is isotropic and obeys Hooke's law, which for any orthogonal coordinate system is given by (Ref. 11, p. 40):

$$\sigma_{ij} = 2\,\mu\,\epsilon_{ij} + \lambda\,\epsilon_{kk}\,\delta_{ij} \tag{7}$$

$$i,j,k = r,\theta,z$$

The σ_{ij} and ϵ_{ij} are the physical stress and strain components, i.e.,

$$\sigma_{rr} = \sigma_r \quad , \quad \sigma_{\theta\theta} = \sigma_\theta \quad , \quad \sigma_{r\theta} = \tau$$

and λ and μ are the Lamé constants:

$$\lambda = \frac{E\nu}{(1+\nu)(1-2\nu)} \quad , \quad \mu = \frac{E}{2(1+\nu)}$$

Strain-Displacement Equations

The strains, in turn, are expressible in terms of the displacements. First we write down the expression for the components of the strain tensor in its most general form (Ref. 12, p. 81):

$$e_{ij} = \frac{1}{2}\left(u_{i|j} + u_{j|i} + u_{k|i}\, u^{k}{}_{|j}\right) \tag{8}$$

where $i, j, k = 1,2,3$; the u_i are the tensor components of the displacement vector and $|j$ denotes the covariant derivative with respect to j. The relationship between covariant and simple derivatives is given by:

$$u_{i|j} = u_{i,j} - \Gamma^{s}_{ij}\, u_s$$

where Γ^{s}_{ij} is the Euclidean Christoffel symbol which in turn is defined in terms of the metric tensor $g^{\alpha\beta}$ (see, e.g., Ref. 5, pp. 34 and 46). The strain tensor in terms of simple derivatives becomes:

$$e_{ij} = \frac{1}{2}\left(u_{i,j} + u_{j,i} + u^{k}_{,j}\right) - \frac{1}{2}\,\Gamma^{s}_{ki}\,\Gamma^{k}_{pj}\,u_{s}\,u^{p} \qquad (9)$$

$$- \frac{1}{2}\left(\Gamma^{s}_{ij}\,u_{s} + \Gamma^{s}_{ji}\,u_{s} - \Gamma^{s}_{kj}\,u^{k}\,u_{s,i} + \Gamma^{s}_{ki}\,u_{s}\,u^{k}_{,j}\right)$$

Since $\Gamma^{s}_{ij} = \Gamma^{s}_{ji}$ and $u^{k} = g^{k\ell}\,u_{\ell}$, we can write e_{ij} in terms of the covariant displacement components only:

$$e_{ij} = \frac{1}{2}\left(u_{i,j} + u_{j,i} + g^{k\ell}\,u_{k,i}\,u_{\ell,j}\right) - \frac{1}{2}\,\Gamma^{2}_{ki}\,\Gamma^{k}_{pj}\,g^{p\ell}\,u_{s}\,u_{\ell} \qquad (10)$$

$$- \frac{1}{2}\left(2\,\Gamma^{s}_{ij}\,u_{s} - \Gamma^{s}_{kj}\,g^{k\ell}\,u_{s,i}\,u_{\ell} + \Gamma^{s}_{ki}\,g^{k\ell}\,u_{s}\,u_{\ell,j}\right)$$

For cylindrical coordinates in particular we have:

$$g^{rr} = 1 \quad , \quad g^{\theta\theta} = \frac{1}{r^{2}} \quad , \quad g^{zz} = 1 \qquad (11)$$

$$\Gamma^{r}_{\theta\theta} = -\,r \quad , \quad \Gamma^{\theta}_{r\theta} = \Gamma^{\theta}_{\theta r} = \frac{1}{r}$$

and all other $g^{\alpha\beta}$ and Γ^{i}_{jk} are zero.

$$U = u_1 \sqrt{g^{rr}} = u_1$$

$$V = u_2 \sqrt{g^{\theta\theta}} = \frac{1}{r} u_2 \tag{13}$$

$$W = u_3 \sqrt{g^{zz}} = u_3$$

$$\epsilon_{ij} = \sqrt{g^{ii}} \sqrt{g^{jj}} \; e_{ij}$$

i, j not summed.

Using Equations (11) and (13) with Equations (12), the physical strain components become:

$$\epsilon_{rr} = U_{,r} + \frac{1}{2}\left(U^2_{,r} + V^2_{,r} + W^2_{,r}\right) + \frac{1}{r} V V_{,r}$$

$$\epsilon_{\theta\theta} = \frac{1}{r}\left(U + V_{,\theta}\right) + \frac{1}{2r^2}\left(U^2_{,\theta} + V^2_{,\theta} + W^2_{,\theta} + V^2\right)$$

$$+ \frac{1}{r^2}\left(UV_{,\theta} - VU_{,\theta} + U^2\right) \tag{14}$$

$$2\epsilon_{r\theta} = \frac{1}{r}\left(U_{,\theta} - V\right) + V_{,r}$$

$$+ \frac{1}{r}\left(U_{,r} U_{,\theta} + V_{,r} V_{,\theta} + W_{,r} W_{,\theta} + (UV)_r\right)$$

Thus after substitution we get for e_{rr}, $e_{\theta\theta}$ and $e_{r\theta}$:

$$e_{rr} = u_{1,r} + \frac{1}{2}\left(u_{1,r}^2 + \frac{1}{r^2} u_{2,r}^2 + u_{3,r}^2\right) - \frac{1}{2r^4} u_2^2 \tag{12}$$

$$e_{\theta\theta} = ru_1 + u_{2,\theta} + \frac{1}{2}\left(u_{1,\theta}^2 + \frac{1}{r^2} u_{2,\theta}^2 + u_{3,\theta}^2\right)$$

$$+ u_1^2 + \frac{1}{2r^2} u_2^2 + \frac{1}{r} u_1 u_{2,\theta} - \frac{1}{r} u_{1,\theta} u_2$$

$$2e_{r\theta} = u_{1,\theta} - \frac{2}{r} u_2 + u_{2,r} + u_{1,r} u_{1,\theta} + \frac{1}{r^2} u_{2,r} u_{2,\theta}$$

$$+ u_{3,r} u_{3,\theta} - \frac{1}{r}\left(u_1 u_2 - u_1 u_{2,r} - u_{1,r} u_2 + \frac{1}{r^2} u_2 u_{2,\theta}\right)$$

Here u_1, u_2 and u_3 are the tensor components of the displacements. The physical components of strains and displacements for the cylindrical coordinate system are given by (Ref. 5, p. 111):

According to von Karman's theory, out of all the non-linear terms only the terms in W make non-negligible contribution. The non-linear terms in U and V are therefore dropped from Equations (14), and the von Karman strain-displacement relations in cylindrical coordinates are obtained:

$$\epsilon_{rr} = U_{,r} + \frac{1}{2} W_{,r}^2$$

$$\epsilon_{\theta\theta} = \frac{1}{r}\left(U + V_{,\theta}\right) + \frac{1}{2r^2} W_{,\theta}^2 \tag{15}$$

$$2\epsilon_{r\theta} = \frac{1}{r}\left(U_{,\theta} - V\right) + V_{,r} + \frac{1}{r} W_{,r} W_{,\theta}$$

The displacement components U, V and W are functions of the three variables r, θ and z. Adopting Kirchhoff's hypothesis that every straight line originally perpendicular to the plate's midsurface remains so after deformation, the displacement vector $\bar{U}(r,\theta,z)$ can be expressed as the sum of a midsurface displacement vector $\bar{u}(r,\theta;\ z=0)$ and a vector $z(\bar{n} - \bar{j}_z)$ (see Appendix A):

$$\bar{U}\left(r,\theta,z\right) = \bar{u}\left(r,\theta\right) + z\left(\bar{n} - \bar{j}_z\right) \tag{16}$$

$$= \left(u - zw_{,r}\right)\bar{j}_r + \left(v - z\frac{w_{,\theta}}{r}\right)\bar{j}_\theta + w\bar{j}_z \ .$$

Therefore,

$$U = u - zw_r \quad ; \quad V = v - z\frac{w_{,\theta}}{r} \quad ; \quad W = w \quad ,$$

and the strain-displacement relationships are finally given by (see also Ref. 12, p. 329):

$$\epsilon_{rr} = u_{,r} + \frac{1}{2}w_{,r}^2 - zw_{,rr}$$

$$\epsilon_{\theta\theta} = \frac{1}{r}\left(u + v_{,\theta}\right) + \frac{1}{2r^2}w_{,\theta}^2 - z\left(\frac{w_{,r}}{r} + \frac{w_{,\theta\theta}}{r^2}\right) \qquad (17)$$

$$2\epsilon_{r\theta} = \frac{u_{,\theta}}{r} + r\left(\frac{v}{r}\right)_{,r} + \frac{1}{r}w_{,r}\,w_{,\theta} - 2z\left(\frac{w}{r}\right)_{,r\theta}$$

The von Karman Plate Equations in Cylindrical Coordinates

Substituting Equations (17) into Equations (4), (5) and (6), we get the stress-displacement relationships:

$$\sigma_r = E'\left\{u_{,r} + \frac{\nu}{r}\left(u + v_{,\theta}\right) + \frac{1}{2}\left(w_{,r}^2 + \nu\frac{w_{,\theta}^2}{r^2}\right) \qquad (18)\right.$$

$$\left. - z\left[w_{,rr} + \frac{\nu}{r}\left(w_{,r} + \frac{w_{,\theta\theta}}{r}\right)\right]\right\}$$

$$\sigma_\theta = E' \left\{ \frac{1}{r}\left(u + v_{,\theta}\right) + \nu u_{,r} + \frac{1}{2}\left(\frac{w^2_{,\theta}}{r^2} + \nu\, w^2_{,r}\right) \right. \tag{19}$$

$$\left. - z\left[\frac{1}{r}\left(w_{,r} + \frac{w_{,\theta\theta}}{r}\right) + \nu\, w_{,rr}\right]\right\}$$

$$\tau = \frac{1-\nu}{2} E' \left\{ \frac{1}{r}\left(u_{,\theta} - v\right) + v_{,r} + \frac{1}{r} w_{,r}\, w_{,\theta} \right. \tag{20}$$

$$\left. - z\,\frac{2}{r}\left(w_{,r\theta} - \frac{w_{,\theta}}{r}\right)\right\} .$$

The loads N_r, N_θ and $N_{r\theta}$ are obtained by integrating the corresponding stresses over the plate thickness:

$$N_r = \int_{-t/2}^{t/2} \sigma_r \, dz \quad ; \quad N_\theta = \int_{-t/2}^{t/2} \sigma_\theta \, dz \quad ;$$

$$N_{r\theta} = \int_{-t/2}^{t/2} \tau \, dz \quad .$$

The results of the above integration are:

$$N_r = E't\left[u_{,r} + \frac{\nu}{r}\left(u + v_{,\theta}\right) + \frac{1}{2}\left(w^2_{,r} + \nu\,\frac{w^2_{,\theta}}{r^2}\right)\right] \tag{21}$$

$$N_\theta = E't \left[\frac{1}{r}\left(u + v_{,\theta}\right) + \nu u_{,r} + \frac{1}{2}\left(\frac{w_{,\theta}^2}{r^2} + \nu\, w_{,r}^2\right)\right] \tag{22}$$

$$N_{r\theta} = \frac{1-\nu}{2} E't \left[\frac{1}{r}\left(u_{,\theta} - v\right) + v_{,r} + \frac{1}{r} w_{,r}\, w_{,\theta}\right] \tag{23}$$

Now substituting Equations (21), (22) and (23) into Equations (1), (2) and (3), the von Karman plate equations for the displacement formulation in cylindrical coordinates are obtained:

$$ru_{,rr} + u_{,r} - \frac{u}{r} + \frac{1-\nu}{2}\frac{u_{,\theta\theta}}{r} + \frac{1+\nu}{2} v_{,r\theta} - \frac{3-\nu}{2}\frac{v_{,\theta}}{r} \tag{24}$$

$$+ rw_{,r}\, w_{,rr} + \frac{1-\nu}{2} w_{,r}^2 + \frac{1+\nu}{2} w_{,r\theta}\frac{w_{,\theta}}{r} + \frac{1-\nu}{2} w_{,r}\frac{w_{,\theta\theta}}{r}$$

$$- \frac{1+\nu}{2}\frac{w_{,\theta}^2}{r^2} = 0$$

$$\frac{1+\nu}{2} u_{,r\theta} + \frac{3-\nu}{2}\frac{u_{,\theta}}{r} + \frac{1-\nu}{2}\left(rv_{,rr} + v_{,r} - \frac{v}{r}\right) + \frac{v_{,\theta\theta}}{r} \tag{25}$$

$$+ \frac{1-\nu}{2} w_{,rr}\, w_{,\theta} + \frac{1+\nu}{2} w_{,r}\, w_{,r\theta} + \frac{1-\nu}{2} w_{,r}\frac{w_{,\theta}}{r}$$

$$+ \frac{1}{r^2} w_{,\theta}\, w_{,\theta\theta} = 0$$

$$\frac{t^2}{12}\nabla^4 w = w_{,rr}\left[u_{,r} + \frac{\nu}{r}\left(u + v_{,\theta}\right)\right] \tag{26}$$

$$+ \frac{1}{r}\left(w_{,r} + \frac{w_{,\theta\theta}}{r}\right)\left[\frac{1}{r}\left(u + v_{,\theta}\right) + \nu u_{,r}\right]$$

$$+ \frac{1-\nu}{r}\left(w_{,r\theta} - \frac{w_{,\theta}}{r}\right)\left[\frac{1}{r}\left(u_{,\theta} - v\right) + v_{,r}\right]$$

$$+ \frac{1}{2} w_{,rr}\left(w_{,r}^{\,2} + \nu \frac{w_{,\theta}^{\,2}}{r^2}\right)$$

$$+ \frac{1}{2r}\left(w_{,r} + \frac{w_{,\theta\theta}}{r}\right)\left(\frac{w_{,\theta}^{\,2}}{r^2} + \nu w_{,r}^{\,2}\right)$$

$$+ \frac{1-\nu}{r^2} w_{,r}\, w_{,\theta}\left(w_{,r\theta} - \frac{w_{,\theta}}{r}\right)$$

This system of equations consists of one fourth-order and two second order elliptic quasilinear partial differential equations. Mathematically, the system can be solved by use of the modern theory of elliptic partial differential equations together with non-linear functional analysis on an appropriately selected Hilbert function space. In the stress formulation, von Karman's equations have been treated by M. S. Berger in Ref. 14, where the buckling load is determined by finding the smallest eigenvalue of an associated linear problem. Of

great importance in the mathematical treatment is the fact that von Karman's equations are derivable from a variational principle.

Another, more practical way to obtain solutions for the three displacements is by use of energy methods. The following chapter discusses the selected energy method of solution and its application to the non-linear problem at hand.

CHAPTER III

PREPARATORY ANALYSIS

Derivation of the Total Potential

Solution for each displacement component will be sought in the form of the product of a power series in the radial variable and a trigonometric series in the circumferential variable. The constant, but unknown, coefficients will be determined by means of the Ritz method. To this purpose, the functional π of the total potential energy can, for the given problem, be most conveniently expressed in terms of cylindrical coordinates. From this functional π, the von Karman Equations (24), (25) and (26) can be derived by setting the first variation of π equal to zero ($\delta\pi = 0$).

The Strain Energy of the Plate

The total potential energy of the plate consists of the strain energy of the plate, U, and of the potential energy Ω of the applied boundary load, i.e.,

$$\pi = U + \Omega \tag{1}$$

The strain energy of the plate is obtained by integrating the strain energy density U_o over the plate volume:

$$U = \iiint_V U_o \, dV \tag{2}$$

As mentioned in Chapter I, the plate material is Hookean isotropic. Now a Hookean material is defined by the condition that its strain energy density is a quadratic function of the strain components. When the Hookean material is also isotropic, its strain energy density will depend only on the magnitude of the principal strains (Ref. 10, pp. 121 and 124):

$$U_o = \frac{1}{2} b_{ij} \epsilon_i \epsilon_j \quad , \quad i, j = 1, 2, 3 \tag{3}$$

The tensor b_{ij} is the material constants tensor:

$$b = \begin{bmatrix} \lambda + 2\mu & \lambda & \lambda \\ \lambda & \lambda + 2\mu & \lambda \\ \lambda & \lambda & \lambda + 2\mu \end{bmatrix},$$

λ and μ being the Lamé constants. Equation (3), written in full, reads:

$$U_o = \frac{1}{2} \lambda \left(\epsilon_1 + \epsilon_2 + \epsilon_3\right)^2 + \mu \left(\epsilon_1^2 + \epsilon_2^2 + \epsilon_3^2\right) \tag{3a}$$

It is necessary to express the strain energy density U_o in terms of the strain components referred to an orthogonal coordinate system, e.g., the cylindrical one.

To this end we write Equation (3a) in terms of the strain invariants I_1 and I_2:

$$U_o = \frac{1}{2} \lambda \, I_1^2 + \mu \left(I_1^2 - 2 \, I_2 \right) \tag{4}$$

Substituting the expressions for the invariants

$$I_1 = \epsilon_1 + \epsilon_2 + \epsilon_3 = \epsilon_{rr} + \epsilon_{\theta\theta} + \epsilon_{zz}$$

and

$$I_2 = \epsilon_1\epsilon_2 + \epsilon_2\epsilon_3 + \epsilon_3\epsilon_1$$

$$= \epsilon_{rr}\epsilon_{\theta\theta} + \epsilon_{\theta\theta}\epsilon_{zz} + \epsilon_{zz}\epsilon_{rr} - \epsilon_{r\theta}^2 - \epsilon_{\theta z}^2 - \epsilon_{zr}^2$$

into Equation (4), we get:

$$U_o = \frac{1}{2} \lambda \left(\epsilon_{rr} + \epsilon_{\theta\theta} + \epsilon_{zz} \right)^2 \tag{5}$$

$$+ \mu \left(\epsilon_{rr}^2 + \epsilon_{\theta\theta}^2 + \epsilon_{zz}^2 + 2 \, \epsilon_{r\theta}^2 + 2 \, \epsilon_{\theta z}^2 + 2 \epsilon_{zr}^2 \right)$$

Equation (5) must be now reduced to the plane stress state. Since U_o is already given in terms of the strain components, it is more expedient to reduce Equation (5) to the plane strain state, and then apply the analogy principle by replacing the material constants λ , μ for the plane strain case by the material constants λ_σ, μ_σ for the

plane stress case (Reference 13, p. 37-2). Setting in Equation (5)

$$\epsilon_{zz} = 0, \qquad \epsilon_{rz} = 0, \qquad \epsilon_{\theta z} = 0$$

and using λ_σ and μ_σ, we get for the plane stress case:

$$U_o = \frac{1}{2} \lambda_\sigma \left(\epsilon_{rr} + \epsilon_{\theta\theta}\right)^2 + \mu_\sigma \left(\epsilon_{rr}^2 + \epsilon_{\theta\theta}^2 + 2\, \epsilon_{r\theta}^2\right) \cdot$$

Using the relations (Reference 13, p. 37-2)

$$\frac{1}{2} \lambda_\sigma = \mu_\sigma \frac{\nu_\sigma}{1 - 2\, \nu_\sigma} \quad , \quad \mu_\sigma = \frac{E_\sigma}{2(1 + \nu_\sigma)} \quad ,$$

$$\nu_\sigma = \frac{\nu}{1 + \nu} \quad \text{and} \quad E_\sigma = E \frac{1 + 2\nu}{(1 + \nu)^2} \quad ,$$

we obtain for λ_σ and μ_σ:

$$\mu_\sigma = \mu \quad ; \quad \frac{1}{2} \lambda_\sigma = \mu \frac{\nu}{1 - \nu} \cdot$$

The final expression for the strain energy density U_o for the plane stress case therefore is (see also Reference 10, p. 161):

$$U_o = \frac{\mu}{1-\nu}\left[\epsilon_{rr}^2 + \epsilon_{\theta\theta}^2 + 2\,\nu\,\epsilon_{rr}\,\epsilon_{\theta\theta} + 2(1-\nu)\,\epsilon_{r\theta}^2\right] \qquad (6)$$

It is convenient to perform the integration in Equation (2) in two steps: first, integrate over the plate thickness t; second, integrate over the doubly connected area of the plate:

$$U = \int_A \int \left[\int_{-t/2}^{t/2} U_o dz\right] dA = \int_A \int T\, dA \qquad (7)$$

Using Equations (17) of Chapter II, Equation (6) for U_o can be rewritten in terms of the displacements and the variable z:

$$U_o = \frac{\mu}{1-\nu}\left[F_1 + F_2 z + F_3 z^2\right]$$

where F_1, F_2 and F_3 represent different groupings of terms in the displacements only. Integration of the above expression over the plate thickness yields:

$$T = \int_{-t/2}^{t/2} U_o dz = \frac{\mu}{1-\nu}\left[F_1 t + \frac{1}{12} F_3 t^3\right]$$

We note that the strain energy per unit area T consists of two parts: the first, linear in t, is the membrane strain energy per unit area, which shall be denoted M; the second, cubic in t, is the bending strain energy per unit area, which shall be denoted B.

We can now write:

$$T = \frac{\mu\, t}{1-\nu} M + \frac{\mu t^3}{12(1-\nu)} B$$

or

$$T = \frac{6D}{t^2} M + \frac{D}{2} B \tag{8}$$

where

$$M = u_{,r}^2 + \frac{1}{r^2}\left(u + v_{,\theta}\right)^2 + \frac{2\nu}{r} u_{,r}\left(u + v_{,\theta}\right) \tag{9}$$

$$+ \frac{1-\nu}{2}\left[\frac{1}{r}\left(u_{,\theta} - v\right) + v_{,r}\right]^2$$

$$+ \frac{1}{r}\left(u + v_{,\theta}\right)\left(\frac{1}{r^2} w_{,\theta}^2 + \nu w_{,r}^2\right)$$

$$+ u_{,r}\left(w_{,r}^2 + \frac{\nu}{r^2} w_{,\theta}^2\right)$$

$$+ (1-\nu)\left[\frac{1}{r}\left(u_{,\theta} - v\right) + v_{,r}\right]\frac{w_{,r}\, w_{,\theta}}{r}$$

$$+ \frac{1}{4}\left(w_{,r}^2 + \frac{1}{r^2} w_{,\theta}^2\right)^2$$

and

$$B = w_{,rr}^2 + \left(\frac{w_{,r}}{r} + \frac{w_{,\theta\theta}}{r^2}\right)^2 \qquad (10)$$

$$+ 2\,\nu\, w_{,rr}\left(\frac{w_{,r}}{r} + \frac{w_{,\theta\theta}}{r^2}\right)$$

$$+ 2(1-\nu)\left(\frac{w_{,r\theta}}{r} - \frac{w_{,\theta}}{r^2}\right)^2$$

and also

$$D = \frac{\mu t^3}{6(1-\nu)} = \frac{Et^2}{12(1-\nu)^2} \quad .$$

The strain energy of the plate now becomes, using Equations (7) and (8),

$$U = \frac{6D}{t^2} \int_A\int M \, dA + \frac{D}{2} \int_A\int B \, dA \qquad (11)$$

or

$$U = U_M + U_B \quad .$$

From Equation (1), the total potential π can be written as

$$\pi = U_M + U_B + \Omega \qquad (12)$$

The Potential of the External Loads

The potential of the applied external loads is given by

$$\Omega = - \int_C \left(\bar{N}_r u + \bar{N}_{r\theta} v \right) ds \qquad (13)$$

The integration is performed along the outer boundary of the plate, i.e., around the circle with radius b, so $ds = b d\theta$ (see Figure 1). Note that for the given problem $\bar{N}_r = 0$ and $\bar{N}_{r\theta}$ on the inner boundary at $r = a$.

The loads $\bar{N}_r$ and $\bar{N}_{r\theta}$ are identical to the loads in an infinite plate due to a uniaxial uniform tension $S[\text{lbs/in}^2]$ (Ref. 8, p. 80):

$$\bar{N}_r = \frac{1}{2} St \left(1 - \frac{a^2}{r^2} \right) \left[1 + \left(1 - 3 \frac{a^2}{r^2} \right) \cos 2\theta \right] \qquad (14)$$

$$\bar{N}_{r\theta} = - \frac{1}{2} St \left(1 - \frac{a^2}{r^2} \right) \left(1 + 3 \frac{a^2}{r^2} \right) \sin 2\theta$$

At the outer boundary $r = b$, therefore, putting $\alpha = \frac{a}{b}$, the loads (14) become:

$$\bar{N}_r = \frac{1}{2} St \left(1 - \alpha^2 \right) \left[1 + \left(1 - 3\alpha^2 \right) \cos 2\theta \right]$$

$$\bar{N}_{r\theta} = - \frac{1}{2} St \left(1 - \alpha^2 \right) \left(1 + 3\alpha^2 \right) \sin 2\theta \quad .$$

We can now write for the potential Ω:

$$\Omega = -\frac{1}{2} \text{Stb} \left(1 - \alpha^2\right) \int_0^{2\pi} \left\{u \left[1 + \left(1 - 3\alpha^2\right) \cos 2\theta\right] - v \left(1 + 3\alpha^2\right) \sin 2\theta \right\} d\theta \tag{15}$$

The displacements u and v in the above integral will be of the form discussed in the section which follows, with b substituted for r in the radial variable.

Selection of Displacement Functions

Approximation functions for the displacement components u, v and w are selected to be of the form:

$$u = a_i h^i_{mn} \rho^m \cos 2(n-1)\theta \tag{16}$$

$$v = b_j h^j_{pq} \rho^p \sin 2q\theta \tag{17}$$

$$w = c_k h^k_{f\ell} \rho^f \cos 2(\ell-1)\theta \tag{18}$$

where a_i, b_j and c_k are the constant but unknown coefficients whose values will be determined by means of the Ritz method. ρ is the radial variable, i.e., a linear function in r. The symbols $h^\alpha_{\beta\gamma}$ are introduced for the purpose of defining the coefficients a_i, b_j

and c_k as single-indexed quantities. The more obvious expression for u, e.g., would be

$$u = a_{mn}\, \rho^m \cos 2(n-1)\theta$$

where summation is performed over m and n. Here the coefficients a_{mn} are double-indexed, i.e., they form an m x n matrix. When writing the matrix equations for the first variation of the total potential, it will be clear that the coefficients a_{mn} must form a column matrix, i.e., they represent a vector in the appropriate vector-space. Instead of converting later the double array a_{mn} into the single array a_i, it is more consistent to start with the single array a_i. The relationship between the two arrays is given below:

$$a_{mn} = a_i h^i_{mn} \,, \quad i \text{ not summed.}$$

There is no summation over i in the above relation because of the unique relationship between i, on one side, and m and n, on the other side. This relationship is as follows:

$$i = m + M(n-1) \tag{19}$$

where M is the upper limit of the range of variation of m (i.e., m = 1,2,3, ..., M). The index n has the range of variation between 1 and N (i.e. n = 1,2,3, ..., N). The relation (19) merely column-lists the two dimensional array a_{mn} into the one-dimensional array a_i.

For every pair (m, n), given within their corresponding ranges of variation, there is one, and only one, i which satisfies Equation (19). Also, for any value of i between 1 and the product M x N, there is a unique set of values for (m, n). Assume, for example, that $m = 1,2,3,4$ and $n = 1,2,3,4,5$. The array on the next page shows the correspondence between i and (m, n). Selecting from it the pair (3, 2) for (m,n), we read for i the number 7; therefore,

$$a_{32} = a_7 \; h^7_{32} = a_7$$

and

$$u^7 = h^7_{32} \; \rho^3 \cos 2(2-1)\theta = \rho^3 \cos 2\theta \; .$$

The u displacement must be symmetric, and the v displacement must be anti-symmetric with respect to the axes $\theta = 0$ and $\theta = \frac{\pi}{2}$. The function for the w displacement is taken symmetric with respect to the same axes. While an anti-symmetric mode for w with respect to these axes is possible, it will correspond to a higher energy level of the system, and thus to a higher critical tensile load, than for the symmetric mode. A substitution in Equations (16), (17) and (18) shows that these conditions are satisfied:

A Numerical Example of Equation (19)

i	m	n
1	1	1
2	2	1
3	3	1
4	4	1
5	1	2
6	2	2
7	3	2
8	4	2
9	1	3
10	2	3
11	3	3
12	4	3
13	1	4
14	2	4
15	3	4
16	4	4
17	1	5
18	2	5
19	3	5
20	4	5

$$u(\rho;\theta) = u(\rho; -\theta) \quad \text{and} \quad u(\rho;\theta) = u(\rho; \pi-\theta) \ ;$$

$$v(\rho;\theta) = -v(\rho; -\theta) \quad \text{and} \quad v(\rho;\theta) = -v(\rho; \pi-\theta) \ ;$$

$$w(\rho;\theta) = w(\rho; -\theta) \quad \text{and} \quad w(\rho;\theta) = w(\rho; \pi-\theta) \ .$$

Determination of the Radial and the Circumferential Variables

From the last paragraph it is evident that our choice for the trigonometric series was appropriate. Setting the angle θ as the circumferential variable satisfies the required conditions for symmetry or anti-symmetry.

The symbols $h^{\alpha}_{\beta\gamma}$ have the value of 1 for all values and combinations of values of the indices α, β and γ. In Equations (16), (17) and (18) the summation is performed over the index α only.

If we rewrite Equations (16), (17) and (18) in the form:

$$u = a_i \, u^i \tag{20}$$

$$v = b_j \, v^j \tag{21}$$

$$w = c_k \, w^k \tag{22}$$

where

$$u^i = h^i_{mn} \, \rho^m \cos 2(n-1)\theta \tag{23}$$

$$v^j = h^j_{pq}\, \rho^p \sin 2q\theta \tag{24}$$

$$w^k = h^k_{f\ell}\, \rho^f \cos 2(\ell-1)\theta \tag{25}$$

it becomes clear why there is no summation over m and n, p and q, and f and ℓ in Equations (16), (17) and (18) or Equations (23), (24) and (25), but there must be summation over i, j and k in Equations (20), (21) and (22). Following the numerical example of Table 1, we have:

$$u = a_1 u^1 + a_2 u^2 + \ldots + a_{19} u^{19} + a_{20} u^{20} .$$

The displacement w must at least satisfy the geometric boundary conditions at the inner and outer boundaries. At the inner boundary (at r = a) there are no geometric conditions to satisfy; the inner boundary is free to deflect and rotate. At the outer boundary (at r = b), there is assumed to be negligible effect from the buckling which occurs at the inner boundary: this buckling is a local phenomenon only and it should not affect the regions of the plate that are distant from the inner coundary. Therefore, at r = b the plate may be assumed to remain flat and undeflected:

$$w(r = b) = 0 \quad \text{and} \quad w_{,r}(r = b) = 0 .$$

The truthfulness of this assumption depends on the ratio $\alpha = a/b$.

The smaller the ratio α is, the better our assumption will be. The closer the ratio α gets to one, the less valid the above assumption becomes: the combination of a non-small α and our assumption of a clamped outer boundary will result in an additional restraining effect which will lead to an increase of the buckling load.

The boundary conditions stated above can be most easily and immediately satisfied if the outer boundary is denoted by $\rho = 0$ and Equation (18) contains powers of ρ no lower than quadratic. The desire to achieve this simplicity therefore leads to the following choice for the radial variable ρ:

$$\rho = 1 - \frac{r}{b} \tag{26}$$

In terms of this variable, the outer boundary will be at $\rho = 0$, and the inner boundary at $\rho = 1 - a/b$ or $\rho = 1 - \alpha$. Thus:

$$w = c_k \, h^k_{f\ell} \, \rho^{f+1} \cos 2(\ell-1)\theta \tag{27}$$

where $k, f, \ell = 1,2,3, \ldots, .$

The expressions for the u and v displacement should include constant terms with respect to ρ, as will be shown in the following section. Equations (16) and (17) now become:

$$u = a_i \, h^i_{mn} \, \rho^{m-1} \cos 2(n-1)\theta \tag{28}$$

$$i, m, n = 1,2,3, \ldots , .$$

$$v = b_j \, h^j_{pq} \, \rho^{p-1} \sin 2q\theta \tag{29}$$

$$j, p, q = 1, 2, 3, \ldots.$$

Derivation of In-Plane Displacements

In the load-deflection curve conceptually shown in Figure 2, the branching point on the S axis corresponds to the onset of buckling, with the plate still maintaining its flat shape. This point on the curve represents the smallest tensile buckling load, S, obtainable from the solution of the associated eigenvalue problem (see Chapter IV). The values of the in-plane displacements u and v included in the solution of this eigenvalue problem should be identical to the values obtained for u^o and v^o from the solution of the problem of the tensioned infinite plate referred to above (Reference 8, p. 80). Later, while solving the non-linear problem, the selected functions for u and v must have the capability of representing the flat plate expressions u^o and v^o as a limiting case. Conversely, the structure of the u^o and v^o equations can indicate or confirm the choice made for radial and circumferential variables. To derive these expressions, we write the inverse of Equations (4),(5) and (6) of Chapter II:

$$\epsilon^o_{rr} = \frac{1}{E}\left(\sigma_r - \nu\sigma_\theta\right) \tag{30}$$

$$\epsilon^o_{\theta\theta} = \frac{1}{E}\left(\sigma_\theta - \nu\sigma_r\right) \tag{31}$$

$$\epsilon^{o}_{r\theta} = \frac{1+\nu}{E}\,\tau \tag{32}$$

where ϵ^{o} indicates the two-dimensional (flat plate) strain. Here σ_r, σ_θ and τ are the stress components for the infinite plate (Reference 8, p. 80):

$$\sigma_r = \frac{1}{2} S \left(1 - \frac{a^2}{r^2}\right)\left[1 + \left(1 - 3\,\frac{a^2}{r^2}\right)\cos 2\theta\right] \tag{33}$$

$$\sigma_\theta = \frac{1}{2} S \left[\left(1 + \frac{a^2}{r^2}\right) - \left(1 + 3\,\frac{a^4}{r^4}\right)\cos 2\theta\right] \tag{34}$$

$$\tau = -\frac{1}{2} S \left(1 - \frac{a^2}{r^2}\right)\left(1 + 3\,\frac{a^2}{r^2}\right)\sin 2\theta \tag{35}$$

The strains ϵ^{o}_{rr}, $\epsilon^{o}_{\theta\theta}$ amd $\epsilon^{o}_{r\theta}$ can be obtained from Equations (17) of Chapter II by dropping the terms in w:

$$\epsilon^{o}_{rr} = u^{o}_{,r}$$

$$\epsilon^{o}_{\theta\theta} = \frac{1}{r}\left(u^{o} + v^{o}_{,\theta}\right) \tag{36}$$

$$2\,\epsilon^{o}_{r\theta} = \frac{1}{r}\left(u^{o}_{,\theta} - v^{o}\right) + v^{o}_{,r}$$

Combining Equations (30), (31) and (32) with Equations (33), (34), (35) and (36) yields a system of three partial differential equations in

u^o, v^o and their first derivatives with respect to the variables r and θ:

$$u^o_{,r} = \frac{S}{2E}\left\{(1-\nu) - (1+\nu)\frac{a^2}{r^2} + \left[(1+\nu) - 4\frac{a^2}{r^2} + 3(1+\nu)\frac{a^4}{r^4}\right]\cos 2\theta \right. \tag{37}$$

$$\frac{1}{r}(u^o+v^o_{,\theta}) = \frac{S}{2E}\left\{(1-\nu) + (1+\nu)\frac{a^2}{r^2} - \left[(1+\nu) - 4\nu\frac{a^2}{r^2} + 3(1+\nu)\frac{a^4}{r^4}\right]\cos 2\theta\right\}$$

$$\frac{1}{r}(u^o_{,\theta}-v^o) + v^o_{,r} = -\frac{S}{4E}\left[(1+\nu) + 2(1+\nu)\frac{a^2}{r^2} - 3(1+\nu)\frac{a^4}{r^4}\right]\sin 2\theta$$

Integrating the above equations and evaluating the constants of integration as necessary, we get:

$$u^o = \frac{Sa}{2E}\left\{(1-\nu)\frac{r}{a} + (1+\nu)\frac{a}{r}\right. \tag{38}$$

$$\left. + \left[(1+\nu)\frac{r}{a} + 4\frac{a}{r} - (1+\nu)\frac{a^3}{r^3}\right]\cos 2\theta\right\}$$

$$v^o = -\frac{Sa}{2a}\left[(1+\nu)\frac{r}{a} + 2(1-\nu)\frac{a}{r} + (1+\nu)\frac{a^3}{r^3}\right]\sin 2\theta \tag{39}$$

Substituting in Equations (38) and (39) for r from Equation (26), i.e., $r = b(1-\rho)$, we get:

$$u^{o} = \frac{SA}{2E}\left\{\frac{1-\nu}{\alpha}(1-\rho) + (1+\nu)\alpha\ \frac{1}{1-\rho}\right. \tag{40}$$

$$\left. + \left[\frac{1+\nu}{\alpha}(1-\rho) + 4\alpha\frac{1}{1-\rho} - (1+\nu)\alpha^{3}\frac{1}{(1-\rho)^{3}}\right]\cos 2\theta\right\}$$

$$v^{o} = -\frac{Sa}{2E}\left[\frac{1+\nu}{\alpha}(1-\rho) + 2(1-\nu)\alpha\ \frac{1}{1-\rho} + (1+\nu)\alpha^{3}\frac{1}{(1-\rho)^{3}}\right]\sin 2\theta \tag{41}$$

The terms in $1/(1-\rho)$ and $1/(1-\rho)^{3}$ in the above equations can be expanded in power series in ρ, since the condition necessary and sufficient for the expansion to exist, $|\rho| < 1$, is always satisfied. The physical meaning of this condition, which can be rewritten as

$$\left| 1 - \frac{r}{b} \right| < 1 \quad \text{or} \quad \frac{r}{b} \neq 0 \ ,$$

is that the plate must be finite (i.e., b can never be infinitely large) and the hole must be present (i.e., $a \neq 0$).

Using the relations:

$$\frac{1}{1-\rho} \cong 1 + \rho + \rho^2 + \ldots\ldots\ldots = \sum_{i=1}^{I} \rho^{i-1}$$

$$\frac{1}{(1-\rho)^3} \cong 1 + 3\rho + 6\rho^2 + 10\rho^3 + \ldots = \sum_{i=1}^{I} \tfrac{1}{2}\, i\,(i+1)\,\rho^{i-1}$$

into Equations (40) and (41), we obtain for u^o and v^o:

$$u^o \cong \frac{Sa}{2E}\left\{ \left(\frac{1-\nu}{\alpha} + (1-\nu)\alpha\right) - \left(\frac{1-\nu}{\alpha} - (1+\nu)\alpha\right)\rho + (1+\nu)\alpha \sum_{i=2}^{I} \rho^i \right. \qquad (42)$$

$$+ \left[\left(\frac{1+\nu}{\alpha}\,(1-\alpha^4) + 4\alpha\right) - \left(\frac{1+\nu}{\alpha}\,(1+3\alpha^4) - 4\alpha\right)\rho \right.$$

$$\left. \left. + \sum_{i=2}^{I}\left[4\alpha - \frac{1}{2}\,(1+\nu)\alpha^3\,(i+1)(i+2)\right]\rho^i \right] \cos 2\theta \right\} \;;$$

$$v^o \cong -\frac{Sa}{2E}\left\{ \left[\frac{1+\nu}{\alpha}\,(1+\alpha^4) + 2(1-\nu)\alpha\right] - \left[\frac{1+\nu}{\alpha}\,(1-3\alpha^4) - 2(1-\nu)\alpha\right]\rho \right. \qquad (43)$$

$$\left. + \sum_{i=2}^{I}\left[2(1-\nu)\alpha + \frac{1}{2}(1+\nu)\alpha^3\,(i+1)(i+2)\right]\rho^i \right\} \sin 2\theta$$

It is easily observed that the above Equations (42) and (43) are completely contained in Equations (28) and (29), including the terms constant with respect to p. The considerations behind the structuring of Equations (28) and (29) are, therefore, completely justified.

CHAPTER IV

SOLUTION

General

The Ritz method is used to solve the non-linear post buckling problem as stated in Chapter I. The unknown displacements u, v and w are assumed to be of a specific form, satisfying at least the geometric boundary conditions, and containing constant but unknown coefficients. The total potential π of the plate-load system is constructed using the assumed expressions for the displacements. This potential π is then made stationary with respect to the unknown coefficients, i.e., the first variation $\delta\pi$ is equated to zero:

$$\delta\pi = \frac{\partial\pi}{\partial a_i}\,\delta a_i + \frac{\partial\pi}{\partial b_j}\,\delta b_j + \frac{\partial\pi}{\partial c_k}\,\delta c_k = 0 \qquad (1)$$

Since the variations δa_i, δb_j and δc_k are arbitrary, the three sets of partial derivatives of π must vanish independently:

$$\frac{\partial\pi}{\partial a_i} = 0\ , \qquad \frac{\partial\pi}{\partial b_j} = 0 \quad \text{and} \quad \frac{\partial\pi}{\partial c_k} = 0 \qquad (2)$$

$$i = 1,2,..,I' \qquad j = 1,2,\ldots,J \qquad k = 1,2,\ldots,K$$

It is convenient to lump together the first two of the above equations, since they involve derivatives w.r.t. the coefficients of the in-plane

displacements. Thus Equation (2) becomes:

$$\frac{\partial \pi}{\partial a_i} = 0 \qquad \text{and} \qquad \frac{\partial \pi}{\partial c_k} = 0 \tag{3}$$

$$i = 1,2,\ldots, I \qquad\qquad k = 1,2,\ldots,K$$

where a_i now includes both the a_i and b_j of Equations (2), with the index i now extended to include the J additional b_j coefficients.

Using Equation (12) of Chapter III with Equation (3), we get:

$$\frac{\partial \pi}{\partial a_i} = \frac{\partial U_M}{\partial a_i} + \frac{\partial U_B}{\partial a_i} + \frac{\partial \Omega}{\partial a_i} = 0$$

and (4)

$$\frac{\partial \pi}{\partial c_k} = \frac{\partial U_M}{\partial c_k} + \frac{\partial U_B}{\partial c_k} + \frac{\partial \Omega}{\partial c_k} = 0$$

From Equations (10) and (15) of Chapter III it can be seen that

$$\frac{\partial U_b}{\partial a_i} = 0 \qquad \text{and} \qquad \frac{\partial \Omega}{\partial c_k} = 0 \quad ,$$

which simplifies Equations (4) as follows:

$$\frac{\partial U_M}{\partial a_i} + \frac{\partial \Omega}{\partial a_i} = 0 \tag{5}$$

$$\frac{\partial U_M}{\partial c_k} + \frac{\partial U_B}{\partial c_k} = 0 \tag{6}$$

These two equations, as will be shown in the following discussion, are essentially a pair of matrix equations. Each equation is a system of I (Equation (5)) or K (Equation (6)) separate equations, but each system can be treated as one matrix equation.

Derivation of the System of Matrix Equations

Let us first treat Equation (5). The partial derivative of the membrane energy (see Chapter III, Equations (9) and (11)) is given by:

$$\frac{\partial U_M}{\partial a_x} = \frac{6D}{t^2} \int_A \int \frac{\partial M}{\partial a_x} \, dA$$

or

$$\left\{\frac{\partial U_M}{\partial a_x}\right\} = \frac{12bD}{t^2} \left[H\right] \left\{a_i\right\} + \frac{6bD}{t^2} \left\{\left(c_{k1} c_{k2}\right)_i\right\} \tag{7}$$

where $\left[H\right]$ is an I x I matrix; $\left\{a_i\right\}$ is the column vector of the a_i unknown coefficients; and $\left\{\left(c_{k1} c_{k2}\right)_i\right\}$ is a column matrix of order I, each term of which contains second order products of c_k, together with definite integrals. The terms of the matrix $\left[H\right]$ consist of definite intergrals only. See Appendix B for the general expression of all the matrices under consideration.

The second term in Equation (5) can be written, using

Equation (15) of Chapter III, as follows:

$$\frac{\partial \Omega}{\partial a_i} = -\frac{1}{2} Sbt \left\{G_i\right\} \tag{8}$$

where $\left\{G_i\right\}$ is a column matrix of order I whose terms are all definite integrals; S is the applied stress. Substituting now Equations (7) and (8) into Equation (5), we obtain:

$$\left[H\right]\left\{a_i\right\} + \frac{1}{2}\left\{\left(c_{k1}c_{k2}\right)_i\right\} = \frac{St^3}{24D}\left\{G_i\right\} \tag{9}$$

Now we can proceed with Equation (6). Using Equation (11) of Chapter III, we can write:

$$\frac{6D}{t^2}\int_A\int \frac{\partial M}{\partial c_k}\, dA + \frac{D}{2}\int_A\int \frac{\partial B}{\partial c_k}\, dA = 0$$

or

$$\frac{12bD}{t^2}\left[M(a_i)\right]\left\{c_k\right\} + \frac{6bD}{t^2}\left\{\left(c_{k1}c_{k2}c_{k3}\right)_k\right\} + \frac{D}{b}\left[B\right]\left\{c_k\right\} = 0 \tag{10}$$

where $\left[B\right]$ is a K x K matrix whose terms are definite integrals; $\left\{c_k\right\}$ is the column vector of the c_k unknown coefficients; $\left\{\left(c_{k1}c_{k2}c_{k3}\right)_k\right\}$ is a column matrix of order k, each term of which contains third order products of c_k, together with definite integrals; and $\left[M(a_i)\right]$ is a K x K matrix whose terms contain definite integrals and are linear in the coefficients a_i.

Equations (9) and (10) are a system of two coupled non-linear matrix equations. This system may be solved by iteration, provided a set of initial values for the a_i and the c_k coefficients is available (see Ref. 15, p. 213), or by successive approximation.

Initial Values for $\{a_i\}$ and $\{c_k\}$

The system of equations to be solved is the one given by Equations (9) and (10) which, with a slight modification, are given below:

$$\left[H\right]\left\{a_i\right\} + \frac{1}{2}\left\{\left(c_{k1}c_{k2}\right)_i\right\} = \frac{St^3}{24D}\left\{G_i\right\} \tag{11}$$

$$\left(\left[M(a_i)\right] + \frac{t^2}{12b^2}\left[B\right]\right)\left\{c_k\right\} + \left\{\left(c_{k1}c_{k2}c_{k3}\right)_k\right\} = 0 \tag{12}$$

Among all possible solutions for a_i and c_k, there is the trivial solution of zero transverse displacement w, or in other words,

$$\left\{c_k\right\} = \left\{0\right\} \quad .$$

In this case, Equation (12) becomes identically zero, while Equation (11) yields a solution for $\left\{a_i\right\}$ which is none other than the flat plate displacement u° and v°, as given in Equations (42) and (43) of Chapter III.

Besides the trivial solution of no transverse displacements, there is the solution, though non-definite, of infinitesimally small transverse displacements, i.e., of infinitesimally small $\left\{c_k\right\}$. In

this case, the term $\left\{\left(c_{k1}c_{k2}\right)_i\right\}$ in Equation (11) is negligible in comparison to the remaining two terms, and also the term $\left\{\left(c_k c_{k2} c_{k3}\right)_k\right\}$ in Equation (12) is negligible in comparison to the term in $\left\{c_k\right\}$. The Equations (11) and (12) are now reduced to the following:

$$\left[H\right]\left\{a_i\right\} = \frac{St^3}{24D}\left\{G_i\right\} \tag{13}$$

$$\left(\left[M(a_i)\right] + \frac{t^2}{12b^2}\left[B\right]\right)\left\{c_k\right\} = 0 \tag{14}$$

The coupled, non-linear system of Equations (11) and (12) is now reduced to two equations of which the first, Equation (13), is independent of the second, Equation (14).

Equation (13) yields a solution of $\left\{a_i\right\}$ in terms of the applied stress S:

$$\left\{a_i\right\} = \frac{St^3}{24D}\left[H\right]^{-1}\left\{G_i\right\}$$

or

$$\left\{a_i\right\} = \frac{St^3}{24D}\left\{A_i\right\} \tag{15}$$

Substituting for $\left\{a_i\right\}$ from the above equation into Equation (14) results in:

$$\left(\frac{St^3}{24D}\left[M(A_i)\right] + \frac{t^2}{12b^2}\left[B\right]\right)\left\{c_k\right\} = 0$$

or

$$\left(\left[M(A_i)\right] + \frac{2D}{Sb^2t}\left[B\right]\right)\left\{c_k\right\} = 0 \tag{16}$$

Equation (16) represents the eigenvalue problem, mention of which was made in the previous chapters. The matrices $\left[M\right]$ and $\left[B\right]$ are real symmetric matrices (see Appendix B), and therefore Hermitian. Since $\left[B\right]$ is also a positive definite matrix, all the eigenvalues ω_k will be real (see Ref. 16, p. 75), where

$$\omega_k = \frac{2D}{Sb^2t} \tag{17}$$

Equation (16) evolves as follows:

$$\left(\left[M(A_i)\right] - \omega\left[-B\right]\right)\left\{c_k\right\} = 0$$

$$\left(\left[-B\right]^{-1}\left[M(A_i)\right] - \omega\left[I\right]\right)\left\{c_k\right\} = 0$$

or

$$\left(\left[X\right] - \omega\left[I\right]\right)\left\{c_k\right\} = 0 \tag{18}$$

where $\left[I\right]$ is the identity matrix and

$$\left[X\right] = \left[-B\right]^{-1}\left[M(A_i)\right]$$

Of significance to us is the largest positive value for ω

which we will denote by ω_o:

$$\omega_o = \frac{2D}{S_o b^2 t}, \quad S_o = \frac{2}{\omega_o} \frac{D}{b^2 t}$$

Modifying:

$$S_o = \frac{2\alpha^2}{\omega_o} \frac{D}{a^2 t} = \lambda_o \frac{D}{a^2 t} \tag{19}$$

For given material and geometry, the largest positive value for ω (i.e., ω_o) will correspond to the smallest positive value for λ(i.e., λ_o), or S(i.e., S_o). Table 1 and Table 2 of Chapter V list values for λ_o (based on one specific set of terms for u and v, see Chapter V), for various combinations and number of terms selected to represent the transverse displacement w, as given by Equation (27) of Chapter III.

The eigenvector corresponding to the eigenvalue ω_o is selected as the starting point for the solution of the non-linear, coupled system of Equations (11) and (12):

$$\text{Eigenvalue } \omega_o \rightarrow \text{Eigenvector } \left\{ {}^{o}_{c_k} \right\} \tag{20}$$

The method of computation of the eigenvalues is described in Chapter V.

Alternatives for the Non-Linear Solution

Systems of non-linear algebraic equations may be solved by means of iteration processes, as shown, for example, in Ref. 15. These processes result in a point by point determination of the curve shown in Figure 2: each set of iterations produces one point, provided convergence is obtained.

It may be possible to reduce large systems of equations to a small number of matrix equations, so as to expedite the solution process by iterating for the matrix unknowns. Equations (11) and (12) represent two such matrix equations, where the scalar unknowns a_i and c_k appear in separate matrices. It might be pointed out, however, that it may be more difficult to obtain convergence for the matrix unknowns than for the scalar unknowns. It may, in fact, be even impossible to obtain convergence at all for the matrix unknowns.

A different approach to the solution of Equations (11) and (12) is to use a successive approximation technique. As for the iteration procedure, the analysis must be developed point by point as successively larger values of load are used to determine the functional dependence of the load on the transverse deflection (i.e., the curve depicted in Figure 2). Both the iteration process and the successive approximation approach are described in detail below.

A more efficient way seems to be a perturbation method. If applicable, it would lead to a functional dependence between load and transverse deflection and thus eliminate the point by point determination of the curve in Figure 2.

An Iteration Process

The eigenvector $\left\{{}^{o}c_{k}\right\}$ as obtained from the computer solution of the eigenvalue problem is normalized w.r.t. the component of largest absolute value. The order of magnitude of $\left\{{}^{o}c_{k}\right\}$ can be further reduced, if necessary for the iteration process. For example:

$$\left\{{}^{1}c_{k}\right\}_{1} = 0.01 \left\{{}^{o}c_{k}\right\}$$

The applied stress S, or the applied stress factor λ, is set at a slightly larger value than S_o, or λ_o, obtained from the uncoupled, linear solution:

$$S: \quad S_1 = 1.01\, S_o \quad \text{or} \quad \lambda: \quad \lambda_1 = 1.01\, \lambda_o \tag{21}$$

Equation (11) becomes

$$\left[H\right]\left\{{}^{1}a_{i}\right\}_{1} + \frac{1}{2}\left\{\left({}^{1}c_{k1}\,{}^{1}c_{k2}\right)_{i}\right\}_{1} = \frac{\lambda_1}{24}\left(\frac{t}{a}\right)^{2}\left\{G_i\right\}$$

or

$$\left\{{}^{1}a_{i}\right\}_{1} = \frac{1}{2}\left[H\right]^{-1}\left(\frac{\lambda_1}{12}\,\frac{t^2}{a^2}\left\{G_i\right\} - \left\{\left({}^{1}c_{k1}\,{}^{1}c_{k2}\right)_{i}\right\}_{1}\right) \tag{22}$$

The vector $\left\{{}^{1}a_{i}\right\}_{1}$ is used in Equation (12) to obtain $\left\{{}^{2}c_{k}\right\}_{1}$:

$$\left(\left[M\left(\frac{1}{a_i}\right)\right] + \frac{\alpha^2}{12}\left(\frac{t}{a}\right)^2 [B]\right)\left\{\frac{2}{c_k}\right\}_1 + \frac{1}{2}\left\{\left(\frac{1}{c_{k1}}\frac{1}{c_{k2}}\frac{1}{c_{k3}}\right)_k\right\}_1 = 0$$

or

$$\left\{\frac{2}{c_k}\right\}_1 = -\frac{1}{2}\left(\left[M\left(\frac{1}{a_i}\right)\right] + \frac{\alpha^2}{12}\left(\frac{t}{a}\right)^2 [B]\right)^{-1}\left\{\left(\frac{1}{c_{k1}}\frac{1}{c_{k2}}\frac{1}{c_{k3}}\right)_k\right\}_1 \qquad (23)$$

Enough iterations with Equations (22) and (23) are performed until the results for $\{c_k\}_1$ and $\{a_i\}_1$ converge.

Having obtained the vector $\{c_k\}_1$ corresponding to S_1, a pair of coordinates (S_1, w_1) results, which represents a point on the load-deflection curve in Figure 2. Any number of such pairs (S_n, w_n) can be obtained for the construction of various load-deflection curves at different locations on the plate. The evaluation of each pair (S_n, w_n) is based on the previously evaluated pair (S_{n-1}, w_{n-1}). Equation (21) becomes:

$$S: \; S_n = 1.01\, S_{n-1} \quad \text{or} \quad \lambda: \; \lambda_n = 1.01\, \lambda_{n-1} \qquad (24)$$

Also, the vector $\{c_k\}_{n-1}$ is used as the initial value (together with the vector $\left\{\frac{1}{a_i}\right\}_n$ obtained from Equation (22) in which λ_n and $\{c_k\}_{n-1}$ have been used) for the evaluation of $\{c_k\}_n$:

$$\left\{\frac{1}{c_k}\right\}_n = \{c_k\}_{n-1} \qquad (25)$$

A Successive Approximation Approach

The successive approximation approach is similar to the iteration approach. It proceeds as follows:

1. The system of Equations (11) is linearized and solved for the a_i's in terms of the applied load S. This corresponds to the plane stress solution of the problem.

2. The results of Step 1 are inserted in the linearized version of Equations (12) to generate an eigenvalue problem.

3. The eigenvalue and appropriately scaled eigenvector of Step 2 are then used in Equations (11) to obtain values of a_i which reflect the effect of lateral deflection.

The equations used in Steps 1, 2 and 3 are given as Equations (26, (28) and (30) below:

$$H_{ji}\, a_i^{(1)} - PG_j = 0 \tag{26}$$

where

$$P = \frac{St^3}{24D} \quad ; \tag{27}$$

$$M_{mik}\, a_i^{(1)}\, c_k^{(1)} + e\, B_{mk}\, c_k^{(1)} = 0 \tag{28}$$

where

$$e = \frac{t^2}{12b^2} = \frac{\alpha^2}{12}\left(\frac{t}{a}\right)^2 \quad ; \tag{29}$$

and

$$H_{ji}\, a_i^{(2)} - P_o G_j + \frac{1}{2}\, g_{jpq}\, c_p^{(1)}\, c_q^{(1)} = 0 \tag{30}$$

where

$$P_o = \frac{S_o t^3}{24D} \quad . \tag{31}$$

The results of the successive approximation analysis are given in Chapter V.

A Perturbation Approach

The theoretical development of a perturbation method, as applied to the non-linear system of Equations (11) and (12), is given in Appendix D of this dissertation.

CHAPTER V

RESULTS

General

All the numerical results given in this chapter were obtained by means of the UNIVAC 1108 computer. Several programs were prepared for the computation of the following phases:

1. Evaluation of the matrices. The elements of each matrix are given as definite integrals (see Appendix B). The integration over the variables ρ and θ was performed exactly (see Appendic C) before the computation, so there was no need for numerical integration, and no accuracy was lost.

2. Inversion of matrices. The inverses of the square matrices $[H]$ and $[B]$ were evaluated by means of an algorithm based on the method of direct operation on rows (Ref. 17, p. 119).

3. Solution of the associated eigenvalue problem. A special program based on the QR Transformation Method (see Ref. 18) was utilized in solving Equation (18) of Chapter IV. This program computes all the roots (i.e., all the eigenvalues) of the equation

$$\text{Det } (X - \omega I) = 0$$

and all the corresponding eigenvectors.

The QR Transformation Method is necessary here because the matrix $[X]$ is non-symmetric. J.G.F. Francis (Ref. 18) developed

this method in analogy to the LR Transformation Method, due to H. Ruthishauser. The QR method is a two step method: first, unitary transformations are developed and applied to the original matrix so that it is rendered into Upper-Hessenberg form; second, successive QR transformations are applied to this matrix so as to force the diagonal elements to converge to the eigenvalues and the sub-diagonal elements to converge to zero.

The Associated Eigenvalue Problem

Table 1 below shows the smallest tensile load parameter λ for various combinations of terms for the w function as given by Equation (18) of Chapter III. The smallest tensile load S is related to λ as follows (see Equation (19) of Chapter IV):

$$S = \lambda \frac{D}{a^2 t}$$

The evaluation of Table 1 was based on an inner-to-outer radii ratio of:

$$\alpha = \frac{a}{b} = \frac{1}{10}$$

and the following representation of u and v: u had 20 power terms and 2 trigonometric terms (of which the first is 1 and the second is $\cos 2\theta$); v had 20 power terms and 1 trigonometric term (i.e., $\sin 2\theta$).

In Table 2, the λ were evaluated based on the same ratio $\alpha = \frac{1}{10}$, but with different u and v representation: both for u

Table 1. Values for λ with $\alpha = 1/10$ and 20 x 2 Terms for u and 20 x 1 Terms for v

Terms for w	Matrix Size	Smallest Positive λ
$f = 2,3$ $\ell = 1,2$	4 x 4	No Positive Value for λ
$f = 2,3,4$ $\ell = 1,2,3$	9 x 9	One Very Large Positive Value for λ
$f = 2,3,4,5$ $\ell = 1,2,3,4$	16 x 16	$\lambda = 49.12$
$f = 2,3,4,5,6$ $\ell = 1,2,3,4$	20 x 20	$\lambda = 45.16$
$f = 2,3,4,5,6$ $\ell = 1,2,3,4,5$	25 x 25	$\lambda = 42.32$
$f = 2,3,4,5,6$ $\ell = 1,2,3,4,5,6$	30 x 30	$\lambda = 41.74$
$f = 2,3,4,5,6,7$ $\ell = 1,2,3,4,5$	30 x 30	$\lambda = 41.64$
$f = 2,3,4,5,6,7$ $\ell = 1,2,3,4,5,6$	36 x 36	$\lambda = 41.22$
$f = 2,3,4,5,6,7$ $\ell = 1,2,3,4,5,6,7$	42 x 42	$\lambda = 41.17$

Table 2. Values of λ with $\alpha = 1/10$

and 10x2 Terms for u and 10x1 Terms for v

Terms for w	Matrix Size	Smallest Positive λ
$f = 2,3$ $\ell = 1,2$	4 x 4	No Positive Value for λ
$f = 2,3,4$ $\ell = 1,2,3$	9 x 9	One Very Large Positive Value for λ
$f = 2,3,4,5$ $\ell = 1,2,3,4$	16 x 16	$\lambda = 47.90$
$f = 2,3,4,5,6$ $\ell = 1,2,3,4$	20 x 20	$\lambda = 43.85$
$f = 2,3,4,5,6$ $\ell = 1,2,3,4,5$	25 x 25	$\lambda = 41.09$
$f = 2,3,4,5,6$ $\ell = 1,2,3,4,5,6$	30 x 30	$\lambda = 40.59$

and v, 10 power terms were taken.

The results obtained for the eigenvalue problem depend upon the results obtained earlier for the prebuckle stress distribution. It is appropriate, therefore, to include here some of the stress distribution results which illustrate the effect of the various types of functional representations used.

Table 3 below shows the effect of ratio $\alpha = a/b$ on the plane stress solution. The exact values of the compressive and tensile stress concentration factors are respectively:

$$SCF_c = -1.00 \quad \text{and} \quad SCF_t = 3.00 \ .$$

Table 3. Effect of $\alpha = a/b$ on the Plane Stress State with 10 x 2 Terms for u and 10 x 1 Terms for v.

$\alpha = a/b$	SCF_c	SCF_t
1/2	-1.0001	3.0001
1/4	-1.0050	3.0056
1/6	-1.0254	3.0372
1/10	-1.0383	3.0601

Tables 4 and 5 which follow show the effect of the number of terms taken for u and v on the plane stress solution, for $\alpha = 1/10$ and $\alpha = 1/20$.

Table 4. Effect of Number of Terms for u and v on the Plane Stress State, with $\alpha = 1/10$

u , v	SCF_c	SCF_t
10 x 2 , 10 x 1	-1.0383	3.0601
12 x 2 , 12 x 1	-1.0277	3.0355
15 x 2 , 15 x 1	-1.0123	3.0144
20 x 2 , 20 x 1	-1.0043	3.0048

Table 5. Effect of Number of Terms for u and v on the Plane Stress State, with $\alpha = 1/20$

u , v	SCF_c	SCF_t
15 x 2 , 15 x 1	-1.0416	3.0649
20 x 2 , 20 x 1	-1.0282	3.0359
25 x 2 , 25 x 1	-1.0211	3.0245
30 x 2 , 30 x 1	-1.0125	3.0142

An examination of Tables 1 and 2 reveals that, as would be expected, the eigenvalues decrease as more terms are taken for w. A comparison of Tables 1 and 2 may appear, however, to be inconsistent with expectation in that the corresponding values of Table 2 are lower than those of Table 1, i.e., the computations involving the smaller total number of terms for u, v and w give lower eigenvalues. This apparent inconsistency can be resolved, however, when it is recognized that the prebuckle stress state associated with the "poorer" plane stress solution likely involves an inplane distribution which simply has lower buckling loads.

Note, however, that the difference in the corresponding results for the two tables is relatively small. This indicates that the use of u and v terms beyond those of Table 2 do not contribute significant improvement. The additional terms, in fact, become a computational liability in the extended nonlinear problem. The numerical errors associated with an increasing number of terms has been documented by Mikhlin (Ref. 19, p. 229).

Comparing the values for λ in either Table 1 or Table 2 with those obtained by G. C. Backer (Ref. 20, p. 54), we observe that Backer's values are consistently lower:

λ from Table 2	λ from Ref. 20, p. 54
47.90	43.74
41.09	40.79
40.59	39.83

This can be attributed to the fact that the plate in Ref. 20 is infinite, while in the present case the plate is finite and clamped at the outer boundary; i.e., a higher value of the critical buckling load would be expected for the finite plate due to the constraining effect of the clamped boundary. A smaller value for α should bring these results into closer agreement. However, to obtain good plane stress representation with a smaller α, a larger number of terms for u and v is necessary, and this leads to the computational difficulties mentioned above.

Tables 6 and 7 list the normalized eigenvectors corresponding to eigenvalues in Tables 1 and 2, respectively.

Solution to the Non-Linear Problem

A solution to the non-linear problem was obtained at the immediate vicinity of the buckling load S_o, using the successive approximation method described in the last section of Chapter IV. The results of this solution are presented in Figures 3 to 5. In obtaining these results, the eigenvalue $\lambda = 47.90$ from Table 2 together with its corresponding eigenvector from Table 7 were used. The number of terms representing the displacements were as follows:

	Terms in ρ	Terms in θ	Total
u	10	2	20
v	10	1	10
w	4	4	16

Table 6. Eigenvectors Corresponding to Eigenvalues in Table 1

Values for $^{o}c_{k}$

λ =	49.12	42.32
1	0.076160	-0.019325
2	-0.488962	0.192353
3	1.0	-0.673795
4	-0.647623	1.0
5	-0.020849	-0.533210
6	0.120016	-0.005208
7	-0.213896	0.044261
8	0.092098	-0.135165
9	-0.000623	0.155589
10	-0.014273	-0.072973
11	-0.006752	-0.002092
12	0.018753	-0.005586
13	-0.012589	0.012545
14	0.024182	-0.020927
15	-0.019150	0.014735
16	0.007108	-0.010255
17		0.040169
18		-0.087010
19		0.094509
20		-0.038001
21		-0.010472
22		0.049162
23		-0.099056
24		0.095959
25		-0.034998

Table 7. Eigenvectors Corresponding to Eigenvalues in Table 2

Values for c_k^o

λ =	47.90	41.09
1	0.076434	-0.019482
2	-0.489620	0.192813
3	1.0	-0.674141
4	-0.647019	1.0
5	-0.018670	-0.533235
6	0.106928	-0.009158
7	-0.190332	0.079025
8	0.079124	-0.239732
9	-0.000549	0.284831
10	-0.016005	-0.129258
11	-0.001475	-0.001036
12	0.014901	-0.013078
13	-0.012499	0.028210
14	0.023914	-0.032130
15	-0.018366	0.016446
16	0.006435	-0.010799
17		0.042646
18		-0.090789
19		0.097185
20		-0.038905
21		-0.010720
22		0.050998
23		-0.103340
24		0.099238
25		-0.036499

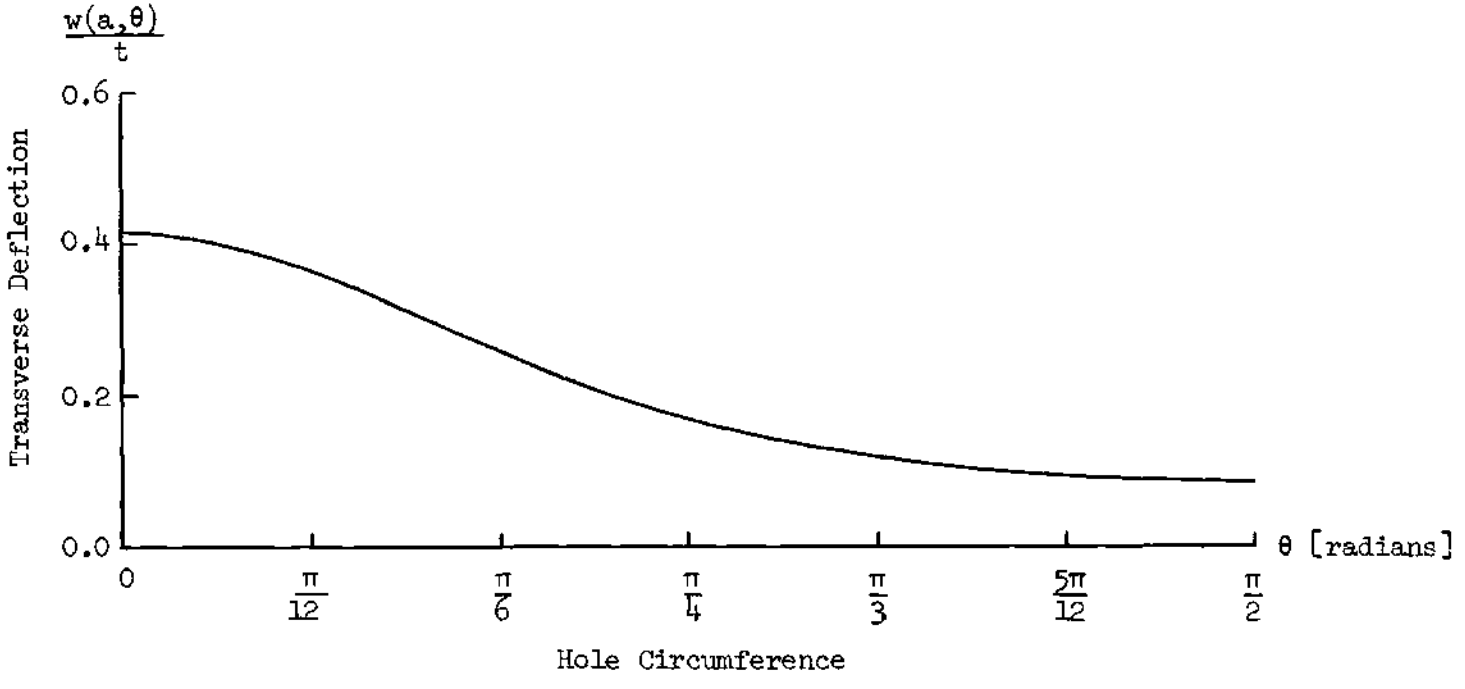

Figure 3. Transverse Deflection at the Hole Boundary

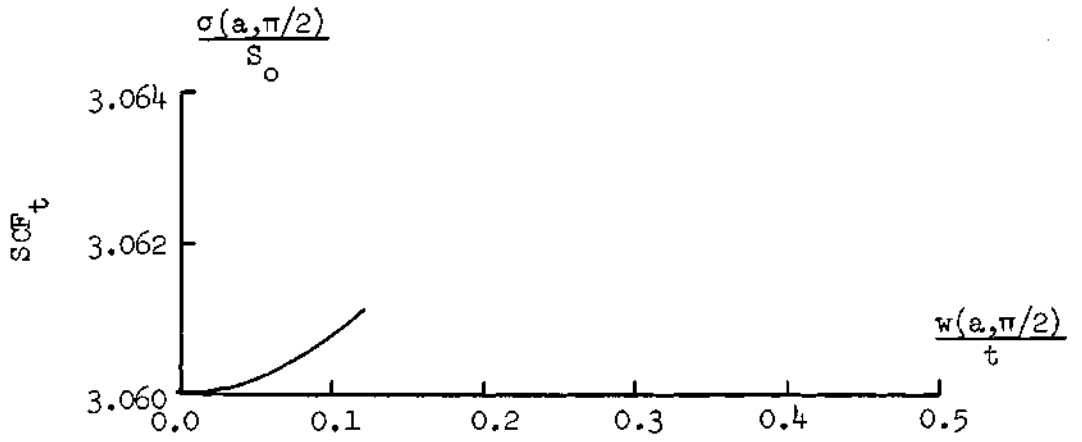

Figure 4. Tensile Stress Concentration Factor vs the Transverse Deflection

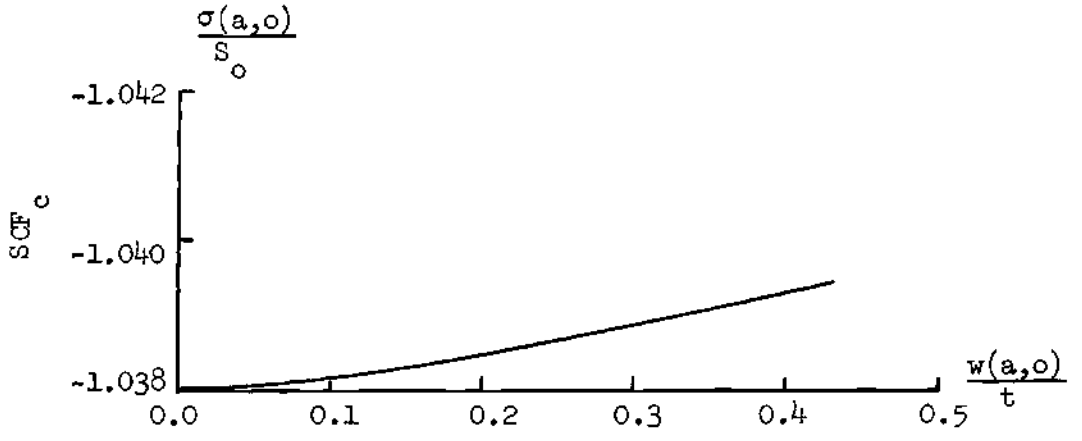

Figure 5. Compressive Stress Concentration Factor vs the Transverse Deflection

The geometry of the plate for which solutions were developed is defined by the ratio values of

$$\alpha = \frac{a}{b} = \frac{1}{10} \qquad \text{and} \qquad \frac{t}{a} = \frac{1}{100} \ .$$

The material was defined by a Young modulus of $E = 10.3 \times 10^6$ psi and a Poisson ratio of $\nu = 0.3333$. These two ratios, which involve three geometric parameters, b, a and t , allow for the full numerical solution of the problem under investigation in terms of one of the above parameters.

Figure 3 shows the mode of the transverse deflections around the hole boundary. Because of the double symmetry, only one quarter of the hole periphery is shown.

The stress concentration factors for a flat infinite tensioned sheet with a circular hole are -1.0 in compression and 3.0 in tension. In our case, for the selected dimensions of $\frac{a}{b} = \frac{1}{10}$, the factors have the values of -1.038 and 3.060. Figures 4 and 5 indicate the manner in which these factors change, as functions of the transverse deflection at the respective location.

As noted earlier, the results obtained here are a first approximation, and they account for transverse deflections in the immediate vicinity of the buckling load. Naturally, the computational process could be extended to obtain results which would be valid for loads greater than the buckling load. Clearly, the development of the load-transverse deflection behavior would, by this successive approximation approach or by the iteration method, involve considerable data processing

and computer time. For this reason only the results presented in Figures 3 to 5 were obtained in the present work. Only the immediate postbuckling trend has been established here. For a more complete description of the postbuckling behavior, a more efficient computational scheme must be developed. Future work on the possibility of developing an efficient and effective perturbation procedure may, for example, prove worthwhile. If such a scheme can be developed, it would appear to possess the possibility of eliminating the point by point computing feature of the methods examined in this dissertation. This might be accomplished by expanding the load S and the displacement coefficients a_i and c_k in terms of a convenient perturbation parameter. A suitable such parameter might, for example, be one of the transverse displacement coefficients (see Appendix D).

Conclusions

The postbuckling behavior at the edge of a circular opening in a large rectangular unidirectionally tensioned sheet was investigated. The non-linear von Karman theory was used in the analysis. The local character of the buckling phenomenon made possible the replacement of the rectangular outer boundary with a circular one, adequately remote from the hole boundary. The process of solution required that an associate eigenvalue problem be solved first. This yielded values for the critical load, which were found to be compatible with values obtained in previous investigation. The lowest tensile buckling load parameter obtained was $\lambda_o = 40.59$. The approximation series for the u, v or w displacements involved the product of a power series

in the radial variable ρ and a trigonometric series in the angle θ.

The flat state of an infinite rectangular sheet with a hole can be best represented by the configuration in Figure 1 if the ratio α of the inner to outer radii is made small. However, the smaller α is, the more terms have to be included in the series representation of the in-plane displacements u and v, and this raises problems of computer accuracy and error accumulation.

For the numerical solution, best results are obtained when the two series, whose product represents the transverse deflection w, have the same number of terms.

Recommendations for Future Research

The postbuckling behavior was determined herein for the eigenvalue associated with $\lambda_o = 47.90$. It is recommended that future work be done to determine the postbuckling behavior associated with lower values for λ_o, e.g., $\lambda_o = 40.59$ or $\lambda_o = 41.09$. This should provide a somewhat improved estimate of the actual postbuckling response at the hole boundary.

The perturbation approach, as discussed elsewhere in this chapter, should be developed and a computational scheme worked out, so that the lengthy point by point determination of the load-deflection curve can be avoided. The choice of a proper perturbation parameter must be given due consideration, since the existence of the Taylor expansion in terms of the perturbation parameter depends on the nature of this parameter.

Results of the kind obtained in this dissertation could be

independently obtained by preparing and solving a finite element model of the plate under consideration. Comparing the results would indicate the relative efficiency and accuracy of the analytic and finite element solutions.

Of great importance would be to perform a series of experiments with large tensioned sheets having a central circular hole, and compare the experimental and the analytical results for the transverse deflection, the stress distribution around the hole and the effect of the postbuckling bending on the stress concentration factors.

APPENDIX A

APPLICATION OF KIRCHHOFF'S HYPOTHESIS TO THE NON-LINEAR PLATE PROBLEM

Let $\bar{r}^o$ be the location radius before the deformation of a point P^o at distance z from the midsurface;

Let $\bar{r}_p^o$ be the location radius before the deformation of the point P_p^o which is the normal projection of the point P^o onto the midsurface:

Let $\bar{r}$ and $\bar{r}_p$ be the location radii after the deformation of P^o and P_p^o, respectively; i.e., point P^o moves to position P and point P_p^o moves to position P_p.

With these definitions, the following equations hold:

$$\bar{r} - \bar{r}^o = \bar{U}(r,\theta,z) \tag{A-1}$$

$$\bar{r}_p - \bar{r}_p^o = \bar{u}(r,\theta;\ z = 0) \tag{A-2}$$

where $\bar{U}$ and $\bar{u}$ are the displacement vectors $\overline{P^oP}$ and $\overline{P_p^oP_p}$ (see Figure A1). The Kirchhoff hypothesis is expressed by:

$$\bar{r} = \bar{r}_p + z\bar{n} \tag{A-3}$$

where $\bar{n}$ is the unit vector normal to the deformed midsurface at

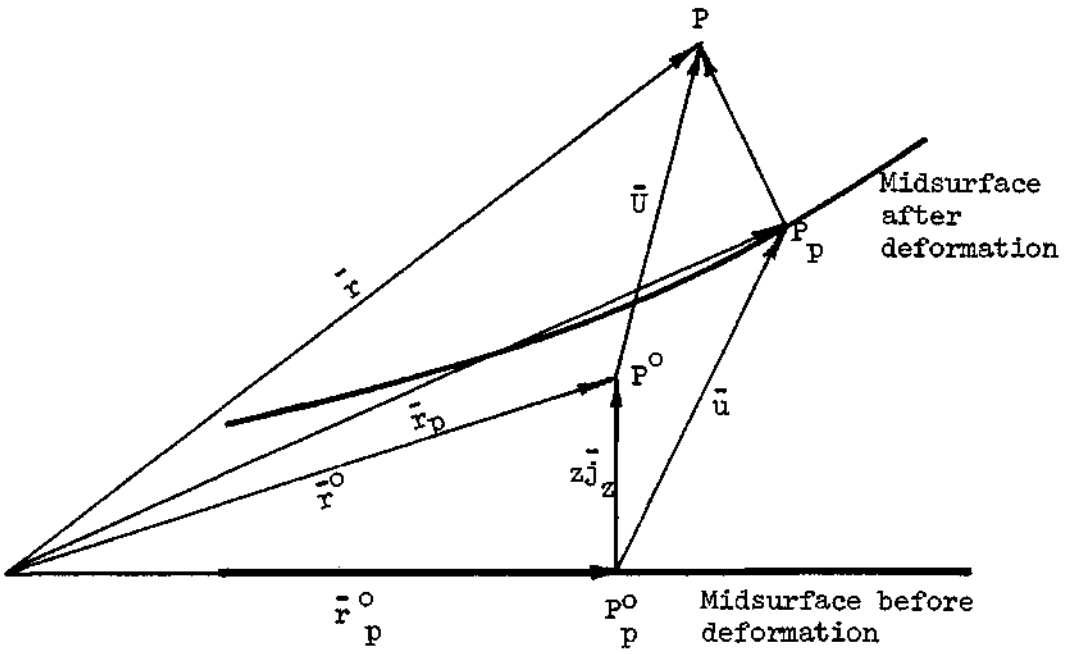

$$\overline{P_p P} = z\bar{n}$$

$$\therefore \bar{U} = \bar{u} + z\left(\bar{n} - \bar{j}_z\right)$$

Figure A1. Kirchhoff's Hypothesis

P_p. Also, from Figure A1 it is obvious that

$$\bar{r}^o = \bar{r}_p^o + z\bar{j}_z \tag{A-4}$$

Substituting Equations (A-3) and (A-4) into Equation (A-2) and then subtracting Equation (A-2) from Equation (A-1), we get:

$$\bar{U}(r,\theta,z) - \bar{u}(r,\theta) = z(\bar{n} - \bar{j}_z) \tag{A-5}$$

The vector $\bar{n}$ is a unit vector defined by

$$\bar{n} = \frac{\bar{N}}{|\bar{N}|} \tag{A-6}$$

where $\bar{N}$ is given by the vector product

$$\bar{N} = \frac{\partial \bar{r}_p}{\partial r} \times \frac{\partial \bar{r}_p}{\partial \theta} \quad . \tag{A-7}$$

The vector $\bar{r}_p$ is given by

$$\bar{r}_p = (r + u)\bar{j}_r + v\bar{j}_\theta + w\bar{j}_z \quad . \tag{A-8}$$

The derivatives of $\bar{r}_p$ will be:

$$\frac{\partial \bar{r}_p}{\partial r} = (1 + u_{,r})\bar{j}_r + v_{,r}\bar{j}_\theta + w_{,r}\bar{j}_z \qquad \text{(A-9)}$$

$$\frac{\partial \bar{r}_p}{\partial \theta} = (u_{,\theta} - v)\bar{j}_r + (r + u + v_{,\theta})\bar{j}_\theta + w_{,\theta}\bar{j}_z$$

Taking the vector product and retaining only terms of the lowest order results in:

$$\bar{N} = - rw_{,r}\bar{j}_r - w_{,\theta}\,\bar{j}_\theta + r\bar{j}_z \qquad \text{(A-10)}$$

Now we need the absolute value of $\bar{N}$:

$$|\bar{N}| = \left(r^2 w_{,r}{}^2 + w_{,\theta}{}^2 + r^2\right)^{\frac{1}{2}}$$

The first two terms are negligible in comparison to the third in the above equation, based on the assumption in Chapter I that $w_{,r} \ll 1$ and $\frac{w_{,\theta}}{r} \ll 1$. Consequently we have

$$|\bar{N}| = r$$

and

$$\bar{n} = - w_{,r}\bar{j}_r - \frac{w_{,\theta}}{r}\,\bar{j}_\theta + \bar{j}_z \quad . \qquad \text{(A-11)}$$

APPENDIX B

EXPRESSIONS FOR THE MATRICES USED IN CHAPTER IV

1. $\left[H\right] = \left[H\right]^T$.

$$\left[H\right] = \left[\begin{array}{c|c} H_{xi} & H_{xi} \\ \hline H_{yi} & H_{yi} \end{array}\right]$$

$$H_{xi} = \int_{\theta=0}^{2\pi} \int_{\rho=1-\alpha}^{0} \left\{ u^x u^i \left[\frac{1}{\rho} \left(\nu m_x + \nu m_i + m_x m_i \right) - \frac{m_x m_i}{\rho^2} - \frac{1}{1-\rho} \right] \right.$$

$$\left. - u^x_{,\theta}\, u^i_{,\theta}\, \frac{1-\nu}{2(1-\rho)} \right\} d\rho d\theta \quad *$$

$$H_{xj} = \int_{\theta=0}^{2\pi} \int_{\rho=1-\alpha}^{0} \left\{ u^x v^j_{,\theta} \left(\frac{\nu m_x}{\rho} - \frac{1}{1-\rho} \right) + u^x_{,\theta}\, v^j_{,\theta}\, \frac{1-\nu}{\rho} \left(\frac{p_j}{\rho} + \frac{1}{1-\rho} \right) \right\} d\rho d\theta$$

---

* If $u = a_i u^i = a_i \rho^m \cos 2(n-1)\theta$, then

$$u_{,r} = -\frac{1}{b}\, u_{,\rho} = -\frac{m}{b}\, \frac{1}{\rho}\, a_i u^i \ .$$

$$H_{yi} = \int_{\theta=0}^{2\pi} \int_{\rho=1-\alpha}^{0} \left\{ v^{y}_{,\theta}\, u^{i} \left(\frac{\nu m_i}{\rho} - \frac{1}{1-\rho} \right) + v^{y} u^{i}_{,\theta} \frac{1-\nu}{2} \left(\frac{p_y}{\rho} + \frac{1}{1-\rho} \right) \right\} d\rho d\theta$$

$$H_{yi} = \int_{\theta=0}^{2\pi} \int_{\rho=1-\alpha}^{0} \left\{ - v^{y} v^{j} \frac{1-\nu}{2} \left[\frac{1}{\rho} \left(p_y + p_j - p_y p_j \right) + \frac{p_y p_j}{\rho^2} + \frac{1}{1-\rho} \right] \right.$$

$$\left. - v^{y}_{,\theta}\, v^{j}_{,\theta} \frac{1}{1-\rho} \right\} d\rho d\theta$$

$$u^{x} = \frac{\partial u}{\partial a_x} \qquad ; \qquad v^{y} = \frac{\partial v}{\partial b_y}$$

$x, i = 1,2,3,\ldots, I'$.

x denotes the specific value of i with respect to which the derivative $\partial/\partial a_i$ is taken.

$y, j = 1,2,3,\ldots, J$.

y denotes the specific value of j with respect to which the derivative $\partial/\partial b_j$ is taken.

H_{xi} is a square $I' \times I'$ symmetric matrix.

H_{yj} is a square $J \times J$ symmetric matrix.

$H_{yi} = H_{jx}$ and $H_{xj} = H_{iy}$.

$m_x, m_i = 1,2,3,\ldots, M$.

$p_y, p_j = 1,2,3,\ldots, P$.

2. $\{G\}$.

$$\{G\} = \{ \quad G_x \quad | \quad G_y \quad \}$$

$$G_x = \left(1 - \alpha^2\right) \int_0^{2\pi} \left[1 + \left(1 - 3\alpha^2\right) \cos 2\theta\right] u^x \, d\theta \quad .$$

$$G_y = - \left(1 - \alpha^2\right) \int_0^{2\pi} \left[\left(1 + 3\alpha^2\right) \sin 2\theta\right] v^y \, d\theta \quad .$$

3. $\{c_{k1}c_{k2}\}$.

$$\{c_{k1}c_{k2}\} = \{(c_{k1}c_{k2})_x \quad | \quad (c_{k1}c_{k2})_y\}$$

$$(c_{k1}c_{k2})_x = \int_{\theta=0}^{2\pi} \int_{\rho=1-\alpha}^{0} \left\{- u^x \left[\frac{w^2_{,\theta}}{(1-\rho)^2} + \nu w^2_{,\rho}\right]\right.$$

$$+ u^x_{,\rho} \left[\left(1 - \rho\right) w^2_{,\rho} + \nu \frac{w^2_{,\theta}}{1-\rho}\right]$$

$$\left. + \frac{1-\nu}{1-\rho} u^x_{,\theta} \, w_{,\rho} \, w_{,\theta}\right\} d\rho d\theta$$

$$\left(c_{k1}c_{k2}\right)_y = \int_{\theta=0}^{2\pi} \int_{\rho=1-\alpha}^{0} \left\{ - v^y_{,\theta} \left[\frac{w^2_{,\theta}}{(1-\rho)^2} + \nu w^2_{,\rho} \right] \right.$$

$$\left. - (1-\nu) \left[\frac{1}{1-\rho} v^y + v^y_{,\rho} \right] w_{,\rho}\, w_{,\theta} \right\} d\rho d\theta$$

4. $\{a\}$.

$$\{a\} = \{\, a_i \mid b_j \,\}$$

5. $\left[M(a)\right] = \left[M(a)\right]^T$.

$$M_{zk} = \int_{\theta=0}^{2\pi} \int_{\rho=1-\alpha}^{0} \left\{ - g_1(1-\rho)\, w^z_{,\rho}\, w^k_{,\rho} - \frac{g_2}{1-\rho} w^z_{,\theta}\, w^k_{,\theta} \right.$$

$$\left. + \frac{1}{2} g_3 \left(w^z_{,\rho}\, w^k_{,\theta} + w^z_{,\theta}\, w^k_{,\rho} \right) \right\} d\rho d\theta \quad .$$

$$g_1 = - u_{,\rho} + \frac{\nu}{1-\rho} \left(u + v_{,\theta} \right) \quad ;$$

$$g_2 = \frac{1}{1-\rho} \left(u + v_{,\theta} \right) - \nu u_{,\rho} \quad ;$$

$$g_3 = (1-\nu) \left(\frac{u_{,\theta} - v}{1-\rho} - v_{,\rho} \right) \quad .$$

$$w^z = \frac{\partial w}{\partial c_z}$$

$z,k = 1,2,3,\ldots, K$

z denotes the specific value of k with respect to which the derivative $\partial/\partial c_k$ is taken.

M_{zk} is a square $K \times K$ symmetric matrix.

6. $\left[B\right] = \left[B\right]^T$.

$$B_{zk} = \int_{\theta=0}^{2\pi} \int_{\rho=1-\alpha}^{0} \Big\{ -(1-\rho)\, w^z_{,\rho\rho}\, w^k_{,\rho\rho} + \nu\left(w^z_{,\rho}\, w^k_{,\rho\rho} + w^z_{,\rho\rho}\, w^k_{,\rho} \right)$$

$$- \frac{1}{1-\rho}\Big[w^z_{,\rho}\, w^k_{,\rho} + \nu\left(w^z_{,\rho\rho}\, w^k_{,\theta\theta} + w^z_{,\theta\theta}\, w^k_{,\rho\rho} \right)$$

$$+ 2(1-\nu)\, w^z_{,\rho\theta}\, w^k_{,\rho\theta} \Big]$$

$$+ \frac{1}{(1-\rho)^2}\Big[w^z_{,\rho}\, w^k_{,\theta\theta} + w^z_{,\theta\theta}\, w^k_{,\rho} - 2(1-\nu)$$

$$\left(w^z_{,\rho\theta}\, w^k_{,\theta} + w^z_{,\theta}\, w^k_{,\rho\theta} \right) \Big]$$

$$- \frac{1}{(1-\rho)^3}\Big[w^z_{,\theta\theta}\, w^k_{,\theta\theta} + 2(1-\nu)\, w^z_{,\theta}\, w^k_{,\theta} \Big] \Big\}\, d\rho\, d\theta$$

7. $\left\{c_{k1}c_{k2}c_{k3}\right\}$.

$$\left(c_{k1}c_{k2}c_{k3}\right)_z = \int_{\theta=0}^{2\pi}\int_{\rho=1-\alpha}^{0}\left\{-w^z_{,\rho}\left[(1-\rho)\,w^3_{,\rho} + \frac{w_{,\rho}w^2_{,\theta}}{1-\rho}\right]\right.$$

$$\left. - w^z_{,\theta}\left[\frac{2w^2_{,\rho}\,w_{,\theta}}{1-\rho} + \frac{w^3_{,\theta}}{(1-\rho)^3}\right]\right\}d\rho d\theta$$

APPENDIX C

INTEGRALS USED IN EVALUATING THE MATRIX ELEMENTS IN CHAPTER IV

1. $$\int \frac{x^m}{1-x}\,dx = -\log(1-x) - \sum_{k=1}^{m} \frac{x^k}{k}$$

$$|x| < 1$$

2. $$\int \frac{x^m}{(1-x)^2}\,dx = m \log(1-x) + \frac{x^m}{1-x} + \sum_{k=1}^{m-1} \frac{m}{k} x^k$$

$$|x| < 1$$

3. $$\int \frac{x^m}{(1-x)^3}\,dx = -\frac{1}{2} m(m-1) \log(1-x) + \frac{x^m}{2(1-x)^2}$$

$$- \frac{mx^{m-1}}{2(1-x)} - \sum_{k-1}^{m-2} \frac{m(m-1)}{2k} x^k$$

$$|x| < 1$$

4. $$\int_0^{2\pi} \cos 2\theta \cos 2(n-1)\theta \, d\theta = \begin{cases} \pi & \text{when } n = 2 \\ 0 & \text{when } n \neq 2 \end{cases}$$

5. $$\int_0^{2\pi} \sin 2\theta \sin 2q\theta \, d\theta = \begin{cases} \pi & \text{when } q = 1 \\ 0 & \text{when } q > 1 \end{cases}$$

6. $$\int_0^{2\pi} \cos 2(n-1)\theta \cos 2(\ell-1)\theta \cos 2(\ell_z - 1)\theta \, d\theta$$

$$= \begin{cases} \frac{\pi}{2} & \text{when } n-1 = |\ell-\ell_z| \text{ or } n-1 = \ell + \ell_z - 2 \\ \pi & \text{when also } \ell = 1 \text{ or } \ell_z = 1 \\ 2\pi & \text{when also } \ell = 1 \text{ and } \ell_z = 1 \\ 0 & \text{otherwise} \end{cases}$$

7. $$\int_0^{2\pi} \cos 2q\theta \cos 2(\ell-1)\theta \cos 2(\ell_z - 1)\theta \, d\theta$$

$$= \begin{cases} \frac{\pi}{2} & \text{when } q = |\ell - \ell_z| \text{ or } q = \ell + \ell_z - 2 \\ \pi & \text{when also } \ell = 1 \text{ or } \ell_z = 1 \\ 0 & \text{otherwise} \end{cases}$$

8. $$\int_0^{2\pi} \cos 2(n-1)\theta \sin 2(\ell-1)\theta \sin 2(\ell_z-1)\theta \, d\theta$$

$$= \begin{cases} \frac{\pi}{2} \text{ when } n-1 = |\ell-\ell_z| \text{ and } n-1 \neq \ell+\ell_z-2 \\ \quad \text{or } n-1 \neq |\ell-\ell_z| \text{ and } n-1 = \ell+\ell_z-2 \\ \pi \text{ when } n=1 \text{ and } \ell=\ell_z \neq 1 \\ 0 \text{ when } \ell=1 \text{ or } \ell_z=1 \\ \quad \text{or otherwise} \end{cases}$$

9. $$\int_0^{2\pi} \cos 2q\theta \sin 2(\ell-1)\theta \sin 2(\ell_z-1)\theta \, d\theta$$

$$= \begin{cases} \frac{\pi}{2} \text{ when } q = |\ell-\ell_z| \text{ and } q \neq \ell+\ell_z-2 \\ \quad \text{or } q \neq |\ell-\ell_z| \text{ and } q = \ell+\ell_z-2 \\ 0 \text{ when } \ell=1 \text{ or } \ell_z=1 \\ \quad \text{or otherwise} \end{cases}$$

APPENDIX D

A PERTURBATION APPROACH

The non-linear equations to be solved are Equations (11) and (12) of Chapter IV, which are given below in tensorial notation:

$$H_{ji}\, a_i + \frac{1}{2}\, g_{jpq}\, c_p\, c_q = P\, G_j \qquad \text{(D-1)}$$

$$M_{mik}\, a_i\, c_k + e\, B_{mk}\, c_k + \frac{1}{2}\, h_{mpqn}\, c_p\, c_q\, c_n = 0 \qquad \text{(D-2)}$$

where

$$P = \frac{St^3}{24D} \qquad \text{and} \qquad e = \frac{1}{12}\left(\frac{t}{b}\right)^2 .$$

The load P and the coefficients a_i and c_k may be expressed in the form of the Taylor expansions in terms of a perturbation parameter ϵ:

$$P = P_o + \epsilon\, P_1 + \epsilon^2\, P_2 + \ldots . \qquad \text{(D-3)}$$

$$a_i = a_i^{(o)} + \epsilon\, a_i^{(1)} + \epsilon^2\, a_i^{(2)} + \ldots . \qquad \text{(D-4)}$$

$$c_k = c_k^{(o)} + \epsilon\, c_k^{(1)} + \epsilon^2\, c_k^{(2)} + \ldots . \qquad \text{(D-5)}$$

Let us associate the perturbation parameter ϵ with the transverse deflection of the plate, and in fact identify it with the first

coefficient c_1, i.e

$$\epsilon = c_1 \tag{D-6}$$

This choice for ϵ implies the following conditions on P, a_i and c_k:

$$P(-\epsilon) = P(\epsilon) \tag{D-7}$$

$$a_i(-\epsilon) = a_i(\epsilon) \tag{D-8}$$

$$c_k(-\epsilon) = -c_k(\epsilon) \tag{D-9}$$

The physical meaning of these conditions is that up and down transverse displacements are equivalent so far as the in-plane load and displacement distributions are concerned (conditions (D-7) and (D-8)), and that the sign reversal of one transverse displacement coefficient (in this case c_1) must involve the sign reversal of all remaining transverse displacement coefficients, in order for the total transverse displacement to switch from an up deflection to a down deflection while preserving its absolute value (condition (D-9)).

Coupling the conditions (D-7), (D-8) and (D-9) to Equations (D-3), (D-4) and (D-5), we get:

$$P = P_o + \epsilon^2 P_2 + \epsilon^4 P_4 + \ldots. \tag{D-10}$$

$$a_i = a_i^{(o)} + \epsilon^2 a_i^{(2)} + \epsilon^4 a_i^{(4)} + \ldots. \tag{D-11}$$

$$c_k = \epsilon\, c_k^{(1)} + \epsilon^3\, c_k^{(3)} + \epsilon^5\, c_k^{(5)} + \ldots. \qquad \text{(D-12)}$$

Equation (D-12) is always true for $k \geq 2$. It can be valid also for the value $k = 1$ if we keep in mind that

$$c_1 = \epsilon \times 1 + \epsilon^3 \times 0 + \epsilon^5 \times 0 + \ldots. \qquad \text{(D-13)}$$

which is the same as

$$c_1^{(1)} = 1 \quad , \quad c_1^{(3)} = c_1^{(5)} = \ldots. = 0 \qquad \text{(D-14)}$$

Obviously, expressions (D-13) and (D-6) are identical.

Substituting now the expressions for P, a_i and c_k from Equations (D-10), (D-11) and (D-12) into the original non-linear Equations (D-1) and (D-2), and then gathering the terms with the same power in the perturbation parameter ϵ, we obtain:

$$\epsilon^0 \left[H_{ji}\, a_i^{(o)} - P_o\, G_j\right] \qquad \text{(D-15)}$$

$$+ \epsilon^2 \left[H_{ji}\, a_i^{(2)} - P_2\, G_j + \frac{1}{2}\, g_{jpq}\, c_p^{(1)}\, c_q^{(1)}\right]$$

$$+ \epsilon^4 \left[H_{ji}\, a_i^{(4)} - P_4\, G_j + \frac{1}{2}\, g_{jpq} \left(c_p^{(1)}\, c_q^{(3)} + c_p^{(3)}\, c_q^{(1)}\right)\right]$$

$$+ \ldots\ldots\ldots = 0$$

$$\epsilon^1 \left[M_{mik}\ a_i^{(o)}\ c_k^{(1)} + e\ B_{mk}\ c_k^{(1)} \right] \qquad \text{(D-16)}$$

$$+ \epsilon^3 \left[M_{mik} \left(a_i^{(o)}\ c_k^{(3)} + a_i^{(2)}\ c_k^{(1)} \right) + e\ B_{mk}\ c_k^{(1)} \right.$$

$$\left. + \frac{1}{2}\ h_{mpqn}\ c_p^{(1)}\ c_q^{(1)}\ c_n^{(1)} \right]$$

$$+ \epsilon^5 \left[M_{mik} \left(a_i^{(o)}\ c_k^{(5)} + a_i^{(2)}\ c_k^{(3)} + a_i^{(4)}\ c_k^{(1)} \right) + e\ B_{mk}\ c_k^{(5)} \right.$$

$$+ \frac{1}{2}\ h_{mpqn} \left(c_p^{(1)}\ c_q^{(1)}\ c_n^{(3)} + c_p^{(1)}\ c_q^{(3)}\ c_n^{(1)} \right.$$

$$\left. \left. + c_p^{(3)}\ c_q^{(1)}\ c_n^{(1)} \right) \right]$$

$$+ \ldots\ldots\ldots = 0$$

Since the magnitude of the parameter ϵ is arbitrary, Equations (D-15) and (D-16) require that each expression in square brackets be equal to zero. If we retain terms of up to the, say, fifth power in ϵ and neglect the remaining terms, the Equations (D-15) and (D-16) will yield a sequence of three pairs of linear algebraic equations in the unknowns P, a_i and c_k (with the exception of c_1).

The <u>first</u> pair of equations is:

$$H_{ji}\ a_i^{(o)} - P_o\ G_j = 0$$

$$\left(M_{mik}\ a_i^{(o)} + e\ B_{mk} \right) c_k^{(1)} = 0 \qquad \text{(D-17)}$$

This system of equations is equivalent to the eigenvalue solution described in Chapter IV (see Equations (13) and (14) of Chapter IV). The solution is performed in three steps.

1. The unknowns $a_i^{(o)}$ are expressed in terms of P_o from the first equation:

$$a_i^{(o)} = P_o \left(H^{-1}_{ji} \, G_j \right) \tag{D-18}$$

2. This expression for $a_i^{(o)}$ is used in the second equation:

$$\left(M_{mik} \, H^{-1}_{ji} \, G_j + \frac{e}{P_o} B_{mk} \right) c_k^{(1)} = 0 \tag{D-19}$$

3. The K x K matrix premultiplying $c_k^{(1)}$ is made singular by solving for the eigenvalues of P_o. The solution relevant to our problem is the least positive eigenvalue of P_o together with its corresponding eigenvector, normalized w.r.t. the first component, i.e., if $c_k^{(1)}$ are the eigenvector components, we will have $c_1^{(1)} = 1$.

The <u>second</u> pair of equations derived from Equations (D-15) and (D-17) is:

$$H_{ji} \, a_i^{(2)} - P_2 \, G_j + \frac{1}{2} g_{jpq} \, c_p^{(1)} \, c_q^{(1)} = 0$$

$$\left(M_{mik} \, a_i^{(o)} + e \, B_{mk} \right) c_k^{(3)} + M_{mik} \, a_i^{(2)} \, c_k^{(1)} \tag{D-20}$$

$$+ \frac{1}{2} h_{mpqn} \, c_p^{(1)} \, c_q^{(1)} \, c_n^{(1)} = 0$$

The steps of the solution of this system of equations are as follows:

1. Express $a_i^{(2)}$ in terms of P_2 from the first equation:

$$a_i^{(2)} = P_2 \left(H_{ji}^{-1} G_j\right) - \frac{1}{2} H_{ji}^{-1} g_{jpq} c_p^{(1)} c_q^{(1)}$$

or

$$a_i^{(2)} = P_2 A_i - \frac{1}{2} A_i' \qquad \text{(D-21)}$$

2. Substitute for $a_i^{(2)}$ into the second equation:

$$Y_{mk} c_k^{(3)} + M_{mik} \left(P_2 A_i - \frac{1}{2} A_i'\right) c_k^{(1)} \qquad \text{(D-22)}$$

$$+ \frac{1}{2} h_{mpqn} c_p^{(1)} c_q^{(1)} c_n^{(1)} = 0$$

where Y_{mk} is the singular K x K matrix from Equation (D - 19):

$$Y_{mk} = M_{mik} a_i^{(o)} + e B_{mk} \quad .$$

3. Recalling from Equation (D-14) that $C_1^{(3)} = 0$, the above Equation (D-22) becomes:

$$Y_{m\alpha} c_\alpha^{(3)} + P_2 \left(M_{mik} A_i c_k^{(1)}\right) - \frac{1}{2} M_{mik} A_i' c_k^{(1)}$$

$$+ \frac{1}{2} h_{mpqn} c_p^{(1)} c_q^{(1)} c_n^{(1)} = 0$$

or

$$Y_{m\alpha}\, c_{\alpha}^{(3)} + P_2\, F_m - F_m' = 0 \quad , \quad \alpha = 2,3, \ldots,k \qquad \text{(D-23)}$$

4. The matrix $Y_{m\alpha}$ is now of K x (K-1) size, and it can be further reduced into a square (K-1) x (K-1) or α x α matrix by separating the first equation implied in the m Equations (D-23):

$$Y_{1\alpha}\, c_{\alpha}^{(3)} + P_2\, F_1 - F_1' = 0 \qquad \text{(D-24)}$$

$$Y_{\beta\alpha}\, c_{\alpha}^{(3)} + P_2\, F_\beta - F_\beta' = 0 \quad , \qquad \text{(D-25)}$$

$$\beta = 2,3, \ldots., K \; .$$

5. The unknowns $c_{\alpha}^{(3)}$ are expressed in terms of P_2 from Equation (D-25):

$$c_{\alpha}^{(3)} = Y_{\beta\alpha}^{-1} \left(F_\beta' - P_2\, F_\beta \right) \qquad \text{(D-26)}$$

The mattix $Y_{\beta\alpha}$ is of one order lower than the singular matrix Y_{mk}. If the matrix Y_{mk} has K different eigenvalues - which is the case in the problem considered in this dissertation - the (K-1) x (K-1) matrix $Y_{\beta\alpha}$ will always be non-singular and, therefore, invertible.

6. Equation (D-26) is inserted into Equation (D-24):

$$Y_{1\alpha}\, Y^{-1}_{\beta\alpha}\left(F'_{\beta}-P_2F_{\beta}\right) + P_2F_1-F'_1 = 0 \quad ,$$

$$P_2\left(F_1-Y_{1\alpha}Y^{-1}_{\beta\alpha}F_{\beta}\right) = F'_1 - Y_{1\alpha}Y^{-1}_{\beta\alpha}F'_{\beta}$$

or

$$P_2\, Q_1 = Q'_1 \quad .$$

Hence

$$P_2 = Q'_1/Q_1 \qquad \text{(D-27)}$$

7. The value of P_2 from Equation (D-27) is used in Equations (D-21) and (D-26) to obtain the values for $a_i^{(2)}$ and $c_\alpha^{(3)}$ respectively.

The <u>third</u> pair of equations, or for that matter, <u>any</u> subsequent pair of equations derived from the Equations (D-15) and (D-17), can be solved in a similar manner for the unknowns:

P_4 , $a_i^{(4)}$, $c_\alpha^{(5)}$ - third pair

P_6 , $a_i^{(6)}$, $c^{(7)}$ - fourth pair

P_{2n-2} , $a_i^{(2n-2)}$, $c^{(2n-1)}$ - nth pair .

REFERENCES

1. Kirsch, G., "Die Theorie der Elasteität und die Berdürfnisse der Festigheitslehre," Zeit, V.D.I., Vol. 42, No. 29, 1898, p. 797.

2. Howland, R.C.J., "On the Stresses in the Neighbourhood of a Circular Hole in a Strip Under Tension," Phil. Trans. Roy. Soc., London, A 229, 1929, p. 49.

3. Adkins, J. E., Green, A. E. and Shield, R. T., "Finite Plane Strain," Phil. Trans. Roy. Soc., A 246, 1953, p. 181.

4. Patel, S. A., Birnbaum, M. R. and Venkatram, B., "Creep Stress Concentration at a Circular Hole in an Infinite Plate," AIAA Journal, Vol. 7, No. 1, January 1969, p. 54.

5. Fung, Y. C., Foundations of Solid Mechanics, Prentice-Hall, Englewood Cliffs, N. J., 1965.

6. Zielsdorff, G. F. and Carlson, R. L., "On Moderately Large Deflection of Multiply Connected Plates," Journal of the Aeronautical Society of India, Vol. 24, No. 4, November 1972.

7. Mindlin, R. D. and Salvadori, M. G., "Analogies," Chapter 16 of Handbook of Experimental Stress Analysis, M. Hetenyi, editor, John Wiley and Sons, Inc., New York, 1950.

8. Timoshenko, S. P. and Goodier, J. M., Theory of Elasticity, McGraw-Hill Book Company, New York, 1961.

9. Ashwell, D. G., "Nonlinear Problems," Chapter 45 of Handbook of Engineering Mechanics, W. Flügge, editor, McGraw-Hill Book Company, New York, 1962.

10. Langhaar, H. L., Energy Methods in Applied Mechanics, John Wiley and Sons, Inc., New York, 1962.

11. Lur'e, A. I., Three-Dimensional Problems of the Theory of Elasticity, Interscience Publishers, New York, 1964.

12. Washizu, K., Variational Methods in Elasticity and Plasticity, Pergamon Press, New York, 1968.

13. Massonnet, Ch., "Two Dimensional Problems," Chapter 37 of Handbook of Engineering Mechanics, W. Flügge, editor, McGraw-Hill Book Co., New York, 1962.

14. Berger, M. S., "On von Karman's Equations and the Buckling of a Thin Elastic Plate," Comm. Pure Appl. Math., Vol. 20, 1967 p. 687.

15. Nielsen, K. L., Methods in Numerical Analysis, The Macmillan Company, New York, 1969, p. 213.

16. Crandall, S. H., Engineering Analysis, McGraw-Hill Book Company, New York, 1956, p. 75.

17. Frazer, R. A., Duncan, W. J. and Collar, A. R., Elementary Matrices, Cambridge, 1963, p. 119.

18. Francis, J.G.F., "The QR Transformation; A Unitary Analogue to the LR Transformation," Parts I and II, The Computer Journal, Vol. 4, October 1961, p. 265 (Part I) and p. 322 (Part II).

19. Mikhlin, S. G., Approximate Methods for the Solution of Differential and Integral Equations, American Elsevier Co., New York, 1967, p. 229.

20. Backer, G. C., "Static and Dynamic Behavior of Tensioned Doubly-Connected Plates," Doctoral Dissertation, Georgia Institute of Technology, Atlanta, Georgia, 1972.

VITA

Abraham S. Hananel was born in May, 1933 in Sofia, Bulgaria. In 1949 he immigrated with his family to the new state of Israel.

Matriculation in 1951 was followed by service in the Israeli Air Force. In 1957 Mr. Hananel graduated from the Israel Institute of Technology with a B.Sc. degree in Mechanical Engineering.

After almost seven years of continuous employment with the Israel Aircraft Industries he left in 1967 for the USA where he joined the Lockheed-Georgia Company. Mr. Hananel participated in the Lockheed-Georgia Graduate Studies Program at the Georgia Institute of Technology and received the M.Sc. degree in Engineering in 1970 and the Ph.D. degree in Aerospace Engineering in January 1974.